



# Suzdalevo Lake (Central Siberia, Russia)—A Tunguska Event-Related Impact Crater?

Radana Kavková<sup>1†</sup>, Daniel Vondrák<sup>2\*†</sup>, Barbora Chattová<sup>3</sup>, Eva Svecova<sup>1</sup>, Marian Takac<sup>1</sup>, Viktor Golias<sup>4</sup>, Richard Štorc<sup>1</sup>, Carlo Stanghellini<sup>5</sup> and Gunther Kletetschka<sup>1,6</sup>

<sup>1</sup>Institute of Hydrogeology, Engineering Geology and Applied Geophysics, Faculty of Science, Charles University, Prague, Czechia, <sup>2</sup>Institute for Environmental Studies, Faculty of Science, Charles University, Prague, Czechia, <sup>3</sup>Department of Botany and Zoology, Faculty of Science, Masaryk University, Brno, Czechia, <sup>4</sup>Institute of Geochemistry, Mineralogy and Mineral Resources, Faculty of Science, Charles University, Prague, Czechia, <sup>5</sup>INAF Istituto di Radioastronomia, Bologna, Italy, <sup>6</sup>Geophysical Institute, University of Alaska Fairbanks, Fairbanks, AK, United States

## OPEN ACCESS

### Edited by:

Felix Riede,  
Aarhus University, Denmark

### Reviewed by:

Dan Hammarlund,  
Lund University, Sweden  
Witold Szczuciński,  
Adam Mickiewicz University, Poland

### \*Correspondence:

Daniel Vondrák  
daniel.vondrak@natur.cuni.cz

<sup>†</sup>These authors have contributed  
equally to this work and share first  
authorship

### Specialty section:

This article was submitted to  
Quaternary Science, Geomorphology  
and Paleoenvironment,  
a section of the journal  
Frontiers in Earth Science

Received: 15 September 2021

Accepted: 24 March 2022

Published: 26 April 2022

### Citation:

Kavková R, Vondrák D, Chattová B,  
Svecova E, Takac M, Golias V, Štorc R,  
Stanghellini C and Kletetschka G  
(2022) Suzdalevo Lake (Central  
Siberia, Russia)—A Tunguska Event-  
Related Impact Crater?  
Front. Earth Sci. 10:777631.  
doi: 10.3389/feart.2022.777631

In 1908, a massive explosion known as the Tunguska Event (TE) occurred in Central Siberia. However, its origin remains widely discussed and environmental impacts are not known in detail. We investigated evidence of the TE in sediments of Suzdalevo Lake, which is located near the explosion epicenter. According to local nomads (Evenkis), Suzdalevo Lake did not exist before the TE and was considered as a possible impact-origin water body. However, apart from oral testimony, there is no evidence of the lake formation process. Two short sediment cores (SUZ1 and SUZ3) were retrieved from the lake and dated using <sup>210</sup>Pb and <sup>137</sup>Cs. The sedimentary record was characterized using magnetic susceptibility, X-ray fluorescence, and the screening for melted magnetic microspherules. To study possible effects of the TE on the lake ecosystem, we performed diatom and freshwater fauna remains analyses. Results indicate that the lake contains sediments that originated before the TE and thus its formation was not related to the impact. Also, the depth to diameter ratio of the lake basin is too low (<1/100) for a young impact crater. In one of the two cores (SUZ1), we documented distinct changes in the lake-catchment ecosystem that occurred within a 5-cm-thick depth interval calculated for the best fit depths for the year 1908 using three alternative age-depth models (CRS, CIC, CFCS), namely, increases in terrestrial matter input (abundant fine plant macroremains, peaks in magnetic susceptibility and the Sr to Rb ratio) and taxonomic diversity and relative abundance of benthic taxa. The shifts in aquatic biota assemblages were likely caused by nutrient supply and improved water column mixing following a catchment disturbance. Nevertheless, precise timing of the observed abrupt changes in relation to the TE is not clear due to uncertainty of the <sup>210</sup>Pb dating method and absence of melted magnetic microspherules or an event layer. The disturbance signals in the proxy data may postdate the TE. Our results demonstrate potential usefulness of the paleolimnological approach to understand the possible environmental consequences of the TE and similar events elsewhere.

**Keywords:** impact structure, airburst, Tunguska cosmic body, forest disturbance, aquatic ecosystems, <sup>210</sup>Pb dating, diatoms, chironomids

## 1 INTRODUCTION

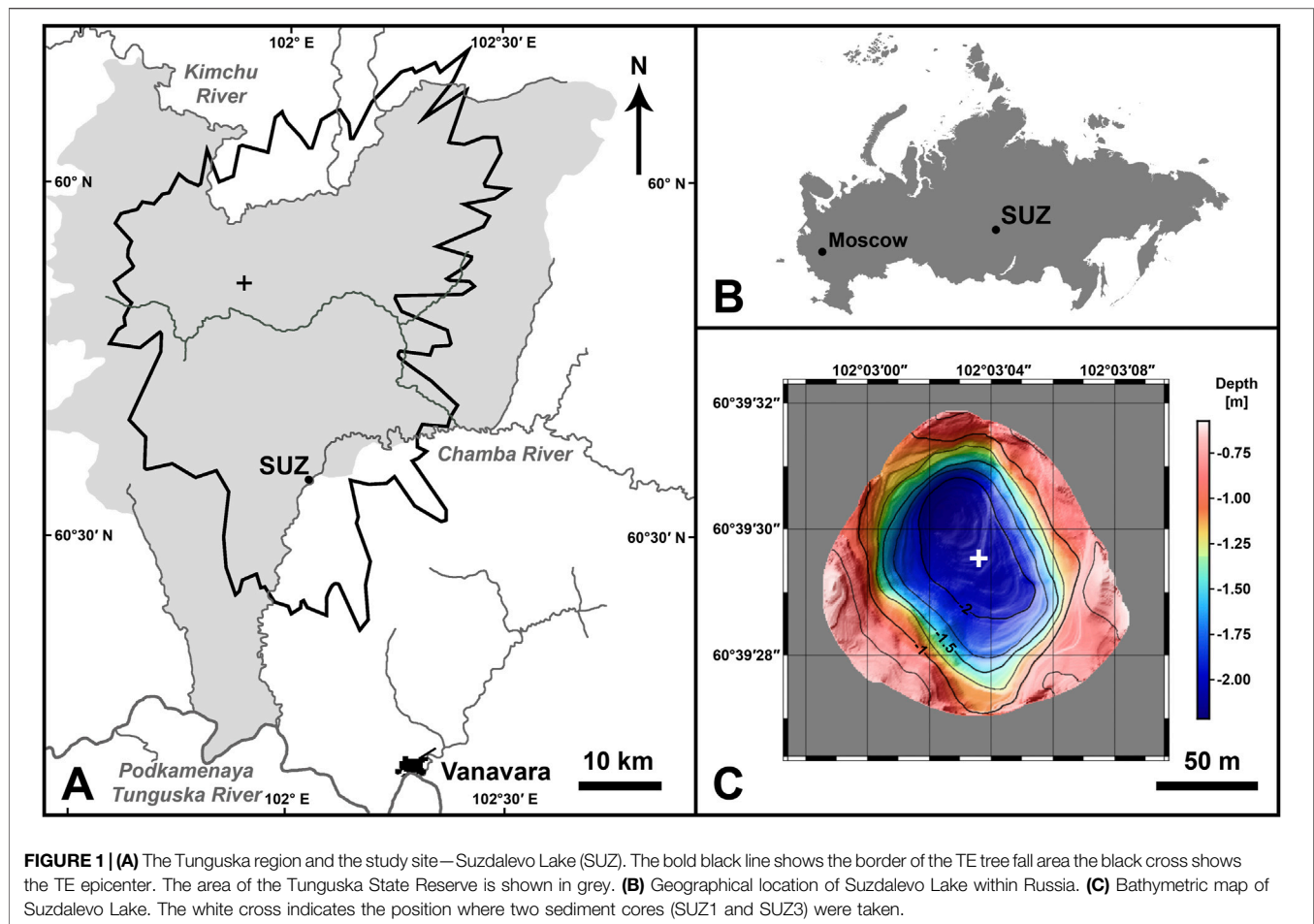
Impact and impact-like events are considered potential triggers of abrupt climatic and environmental changes, as their direct destructive power influences atmospheric and geochemical processes on local as well as global levels (Covey et al., 1994). Their potential consequences include not only earthquakes, tsunamis, and fires, but also processes such as dust loading, ozone depletion, sulfate aerosol formation, disturbances of Earth's magnetic field, and nitric acid rain (Turco et al., 1981; Kolesnikov et al., 1997; Toon et al., 1997; Shishkin 2007; Wünnemann and Weiss 2015; Artemieva and Shuvalov 2016). On the morning of 30th June 1908, a massive explosion occurred in Central Siberia, near the Podkamennaya Tunguska River, in the Evenkiysky District, Russia (e.g., Gladysheva, 2020a; Gladysheva, 2020b and references therein). The explosion affected an area of about 2,000 km<sup>2</sup> of continental taiga and uprooted more than 80 million trees with an estimated power equivalent to 20–30 million tons (Mt) of TNT (Rosanna et al., 2015; Artemieva and Shuvalov 2016; Robertson and Mathias 2019). It was likely the most destructive impact-like event witnessed in the modern history of humankind. Fortunately, the Tunguska Event (TE) epicenter was located in a very remote and sparsely populated region. At least three people (local Evenki nomads) died as a direct consequence of the TE, and an unknown number of people were injured from the effects of the shockwave, thermal radiation, or glass damage (Jenniskens et al., 2019). A much smaller explosion (~0.5 Mt of TNT) from a meteorite about 19 m in diameter caused injuries of ~1,600 people on 15th February 2013 in a more populated area in the Chelyabinsk Oblast, Russia (Brown et al., 2013; Kletetschka et al., 2015; Kartashova et al., 2018), documenting the destructive potential of such extreme events. TE-related glass damage was reported over a wide area, especially around the Angara River, even 400 km away from the explosion epicenter (Jenniskens et al., 2019). The night sky shone brightly for a few days over an even larger area, including Europe. The origin of this phenomenon was explained by the same mechanism as the formation of noctilucent clouds, with water and dust creating ice crystals at heights from 70 to 300 km in the atmosphere. The reflective surface of these TE noctilucent clouds was 10<sup>4</sup>× greater than usual, probably caused by a two to three orders of magnitude larger crystal size (Gladysheva 2012).

The TE is considered to have been caused by the impact of a cosmic body, but neither an impact crater nor any stony fragments have been found (Artemieva and Shuvalov 2016). An exotic quartzitic boulder, known as John's Stone, was hypothesized by some authors as a potential meteorite, possibly of Martian origin, but research by Bonatti et al. (2015) suggested its relation to the local Permian-Triassic Trap magmatism-hydrothermalism. In recent years, several lines of evidence have been published in support of the hypothesis that Cheko Lake (~10 km NW of the inferred TE epicenter) fills an impact crater created by a fragment of the parent TE cosmic body. These include geophysical data (e.g., Gasperini et al., 2007; Gasperini 2015), the presence of tree trunks and branches below lake sediments (Gasperini et al., 2014), and

physical modelling (Foschini et al., 2019). However, this hypothesis was questioned by Collins et al. (2008) and Rogozin et al. (2017) based on theoretical models and sediment dating, respectively. According to local Evenki reindeer-herding nomads (Evgeniya Karnouchova, pers. comm.), a TE-related origin is also assumed for Suzdalevo Lake, a small water body located in the southern part of the tree fall area, as it was first mapped by expeditions after the TE (Vasilyev 1998; Jenniskens et al., 2019, and references therein). Today, more than 110 years after the explosion, many doubts and uncertainties persist about the TE. As the original asteroid hypothesis was called into question due to the absence of a meteorite fragment, a cometary origin of TE has been suggested by some authors (e.g., Kresák 1978; Gladysheva, 2020a; Gladysheva, 2020b). However, other causes (e.g., the volcanic ejection of natural gas, a dark matter collision, solar activity) have been discussed as well (Kundt 2001; Froggatt and Nielsen 2015; German 2019). In a recent paper, Khrennikov et al. (2020) argue that the TE was caused by an iron asteroid body, which passed through the atmosphere at a minimum altitude of 10–15 km with trajectory length about 3,000 km and continued to the near-solar orbit.

Overall knowledge of the TE is limited due to the lack of scientific observations at the time of the explosion and almost no research on the epicenter performed in the following two decades. Moreover, most of the later investigations were conducted to determine what phenomenon caused the TE, with much less attention paid to the topic of environmental damage. Natural archives, such as tree rings, peat, and especially lake sediments, have the great potential to provide important new evidence of this kind.

Only a few studies on these natural archives in the Tunguska region have been performed so far. Tree-ring research by Kletetschka et al. (2017) revealed a directional chemical response in the xylem of larch (*Larix*) trees that survived the TE inside the tree fall area. Badyukov et al. (2011) described the presence of metal microspherules consisting of Ni(Cr) bearing wüstite and magnetite with Ni-rich metal inclusions and glassy silicate microspherules in soils above the floodplain of the Chunya River, which may indicate the possible presence of cosmic body material in various sedimentary natural archives. Similar findings of microspherules were reported much earlier by Zaslavskaya et al. (1964). Lake sediments have been rarely studied, as the location is very remote, and lakes are not common in the area. An important contribution was provided by investigations of the Zapovednoe Lake sedimentary record. Despite its location outside of the tree fall area and the radiant burn area (60 km from the TE epicenter; Johnston and Stern 2019 and references therein), the lake sediment contained a characteristic yellowish (clayey) TE layer possibly caused by an earthquake and likely related catchment erosion (Kletetschka et al., 2019a; Darin et al., 2020). A considerable increase in magnetic susceptibility followed immediately after the deposition of this TE layer, pointing to intense fires near the TE epicenter. These fires (e.g., Svetsov 2002; Jenniskens et al., 2019) could converted non-magnetic iron in organic material into magnetite particles with high magnetic susceptibility that



were then incorporated into ash and deposited in soils and various sediments (Kletetschka and Banerjee 1995; Kletetschka et al., 2019a). Therefore, such a characteristic signal should also be present in other lake sediment records and peat sequences in the region. A similar clayey layer of TE age has already been found in Cheko Lake sediments (Gasperini et al., 2009). If combined with a paleoecological approach, the presence of characteristic TE layers should enable studies on the effects of the event on related ecosystems. The potential of such paleoecological methods has already been demonstrated by Tositti et al. (2006) who discovered TE-related anomalies in tree pollen productivity and the onset of a phase of more humid conditions at the Raketka peat bog site (8 km from the TE epicenter). Other peat profiles (sites located 6–65 km from the TE epicenter; plant material of *Sphagnum fuscum*) have revealed probable traces of acid rains as a reaction to the TE, as evidenced by a positive anomaly in  $\delta^{15}\text{N}$  (Kolesnikov et al., 1998).

In this study, we present a paleoenvironmental record of Suzdalevo Lake sediments. As Suzdalevo Lake has been reported by local Evenki people to have appeared just after the TE, we assumed that the lake could be a TE impact crater and/or an important natural archive to investigate the disturbance of the taiga forest and related changes in the aquatic environment. Reconstructing local environmental changes caused by the TE

is crucial to understanding the processes triggered by this unique phenomenon.

## 2 REGIONAL GEOLOGICAL SETTING AND THE STUDY SITE

The TE tree fall area of butterfly shape (axis along the  $115^\circ$  azimuth; **Figure 1A**) is located in the Tunguska Basin, which is in the western part of the Siberian craton that is composed of high-grade Archean metamorphic complexes and granites (Gladkochub et al., 2006; Artemieva and Shuvalov 2016). At the Permian-Triassic boundary ( $\sim 251$  Ma), the area was affected by the extensive eruption of Siberian flood-volcanic rocks, the largest subaerial volcanic event known ( $\sim 7 \times 10^6$  km<sup>2</sup> buried by basalts) (Kamo et al., 2003). Recent local river basins are filled with Quaternary sediments (fluvial and aeolian deposits) and soils, which also applies to the surroundings of the study site. Permafrost is discontinuous in this area with thickness up to 25 m (Gasperini et al., 2007; Ponomarev et al., 2019). Distinct climatic changes have been observed in overall central Siberia over the last century. The climate has become much warmer, and in some regions dry summer conditions have prolonged the “no-rain” period. This increases the likelihood of extremely dry periods and

the risk of extreme fire events (Tchebakova et al., 2011). At the nearest meteorological station, that is placed in Vanavara (60°20'45"N 102°16'54"E; **Figure 1A**), the current (period 2000–2020) mean annual temperature is  $-4.5^{\circ}\text{C}$ , the mean January temperature  $-27.7^{\circ}\text{C}$ , and the mean July temperature  $17.8^{\circ}\text{C}$ . The “normal” mean annual precipitation (period 1933–2020) is 421 mm, however, the minimum mean annual precipitation of 271 mm was observed in 2016 (Weather and Climate 2021).

Suzdalevo Lake is a shallow water body located very close to the Chamba River (60°39'29.05"N, 102°3'3.36"E) a tributary of the Podkamennaya Tunguska River, 20 km SW from the TE epicenter (i.e., inside the tree fall area; **Figure 1A**). The lake is separated from the Chamba River by a natural dike  $\geq 45$  m wide and  $\geq 4$  m high. No bathymetric measurements or limnological characterizations of this site have been previously published. The lake was allegedly named after K. I. Suzdalev, a merchant from Vanavara, who visited the site shortly after the TE (Evgeniya Karnouchova, pers. comm.). Vegetation in the lake catchment is characterized by mixed taiga consisting mostly of pine (*Pinus*), birch (*Betula*), spruce (*Picea*), willow (*Salix*), and Dahurian larch (*Larix gmelini*) trees, with undergrowth of blueberries (*Vaccinium myrtillus*), cranberries (*Vaccinium vitis-idaea*), mosses and lichens. No historical logging at this site is known.

## 3 METHODS

### 3.1 Morphobathymetric Characterization of the Study Site

In May 2019, we surveyed the lake with a close-spaced grid of echosounding lines, with the aim to compile a morphobathymetric map of its floor and identify a suitable position for sediment coring. We used techniques and instruments like those employed by Gasperini et al. (2007) at Cheko Lake. The bathymetric measurements were performed with a 200 kHz echosounder tied to a wooden stick aside of a boat while a transducer was located at about 30 cm below the water surface. Instead of acquiring only the depth value provided by the echosounder through the serial port, we collected the entire echogram by means of a 16 bit A/D converter driven by SwanPRO acquisition software. The acquisition parameters of the echosounder signal were as follows: sample rate 0.856  $\mu\text{s}$ , trace length 25 ms, and 2,140 trace samples (seven traces per second). The collected data were stored in XTF format, converted to SEG Y format, consistency was checked using the Segy-change preprocessing software program (Stanghellini and Carrara 2017), and processed using SeisPrho software program (Gasperini and Stanghellini 2009) to display echograms and semi-automatically digitize the sediment-water interface. The lake-floor profiles were subsequently corrected for the vertical offset between the water surface and the transducer vertical position, and then exported in ASCII (lon, lat, z) format. The file was then processed with GMT to produce both a regular grid file and the final map. The original data were affected by spatial noise due to GPS precision being limited to about 1 m. To reduce

this spatial noise, the final morphobathymetric map was compiled using a 2D median filter with a searching radius of 10 m.

### 3.2 Core Retrieval, Sediment Lithology

During the same field survey, two short lake sediment cores, SUZ1 and SUZ3, were collected using a Kajak gravity corer (sampling tube diameter of 5.8 cm and length of 50 cm) from the deepest middle part of Suzdalevo Lake. The lengths of the obtained cores SUZ1 and SUZ3 were 42 and 46 cm, respectively. Both cores were immediately sliced in steps of 1 cm, with the uppermost 1 cm (0–1 cm) divided into two layers—0–0.5 cm and 0.5–1 cm. The color, grain size, and amount of plant macroremains (qualitative data) were recorded during slicing and during analyses of aquatic biota remains.

### 3.3 Short-Lived Isotope Dating

Both sediment cores were measured using gamma spectroscopy for the specific activity of  $^{210}\text{Pb}$ ,  $^{137}\text{Cs}$ , and  $^{226}\text{Ra}$  isotopes in the Radiometry Laboratory (Institute of Geochemistry, Mineralogy and Mineral Resources Charles University, Prague, Czechia). Individual samples (1-cm-thick layers; the two uppermost layer were merged) were measured by well-in-well geometry in a SILAR<sup>®</sup> low-background anti-Compton-anti-coincidence gamma spectrometer with a specially designed 40 × 40 mm Na(Tl) well-type LEADMETER<sup>®</sup> detector with a total efficiency of 46.2% (for  $^{210}\text{Pb}$  line of 47 keV) placed in a well-type guard NaI(Tl) detector 160 × 125 mm in 10-cm-low-background lead shielding (Hamrová et al., 2010). A Canberra DSA 2000 multichannel analyzer controlled by GENIE 2000 software was used to determine the specific activities of the above-mentioned isotopes. The measuring time for individual samples was 2 days, and 6 days for background. Special in-house standards with a light matrix were used for radionuclide quantification in the same geometry of the 8 ml vials. The IAEA-447 standard (moss-soil) was used as  $^{210}\text{Pb}$  reference material with a result of  $340 \pm 6 \text{ Bq kg}^{-1}$  for the recommended value of  $338 \text{ Bq kg}^{-1}$  and corrected for decay from the reference date (15/11/2009). Due to low weights of the SUZ1 samples affecting the results, we decided to measure isotope activities also for the SUZ3 core by merging four adjacent 1-cm-thick layers in a row. The output from the heavier 4-cm-merged samples (~4 g of dry sediment) was expected to be more accurate. The age of individual layers was obtained using the Constant Rate of Supply (CRS), the Constant Initial Concentration (CIC), and the Constant Flux Constant Sedimentation rate (CFCS) age-depth models that are implemented in an R package “serac” (Bruel and Sabatier 2020 and references therein). These alternative models were used because none of them can be considered as a universal method of age-depth model construction.

### 3.4 Sediment Magnetism and Geochemistry

All sediment samples from both cores were placed into plastic cups and magnetic susceptibility was measured using a SM30

magnetic susceptibility meter (ZHinstruments Inc., Czechia) at an oscillation frequency of 8 kHz and generated magnetic field amplitude of 40 A/m. The magnetic susceptibility values [X (SI), average of three measurements] were mass normalized.

The total content of selected elements was determined by means of X-ray fluorescence (XRF) spectrometry using a handheld ED-XRF analyzer VANTA VMR with a Silicon Drift Detector (Olympus, United States). The ED-XRF analyzer was coupled with a programmable moving core holder and autonomously run by a computer (for details Kletetschka et al., 2018; Kletetschka et al., 2019b). National Institute of Standards and Technology (NIST) standard reference materials 2711a Montana II Soil and 2710a Montana I Soil were used for quality control. Finally, we focused on an interpretation of concentrations and ratios of individual elements that are likely relevant to tracking the history of the lake's productivity as well as the erosional activity in the lake catchment. The strontium to rubidium ratio (Sr/Rb) and titanium (Ti) concentration were selected as proxies characterizing the input of material from the catchment (Cuven et al., 2010; Xu et al., 2010), phosphorus (P) and the silicon to zirconium ratio (Si/Zr) as proxies of lake productivity (Cuven et al., 2011), and the iron to manganese ratio (Fe/Mn) with iron (Fe) concentration control as proxy of near bottom redox conditions (Mackereth 1966; Davison 1993).

### 3.5 Separation and Analyses of Magnetic Microspherules

For separation of magnetic microspherules from the sediment samples (all SUZ1 layers), we performed a standard separation technique described by Israde-Alcántara et al. (2012). The separated material was analyzed under a dissecting optical microscope at 25–70× magnification. Suspected spheric objects (diameter >3 μm) were manually placed on aluminum stubs with nonmagnetic tools (sharpened wooden sticks). Finally, the spheric objects were identified with a scanning electron microscope (SEM) TESCAN Vega in back-scattered electron (BSE) and secondary electron (SE) modes, and subsequent elemental microanalysis was conducted using an energy dispersive X-ray spectroscope (EDS, detector X-Max 50; Oxford Instruments, United Kingdom) at the Laboratory of Scanning Electron Microscopy (Institute of Petrology and Structural Geology, Faculty of Science, Charles University, Prague, Czechia).

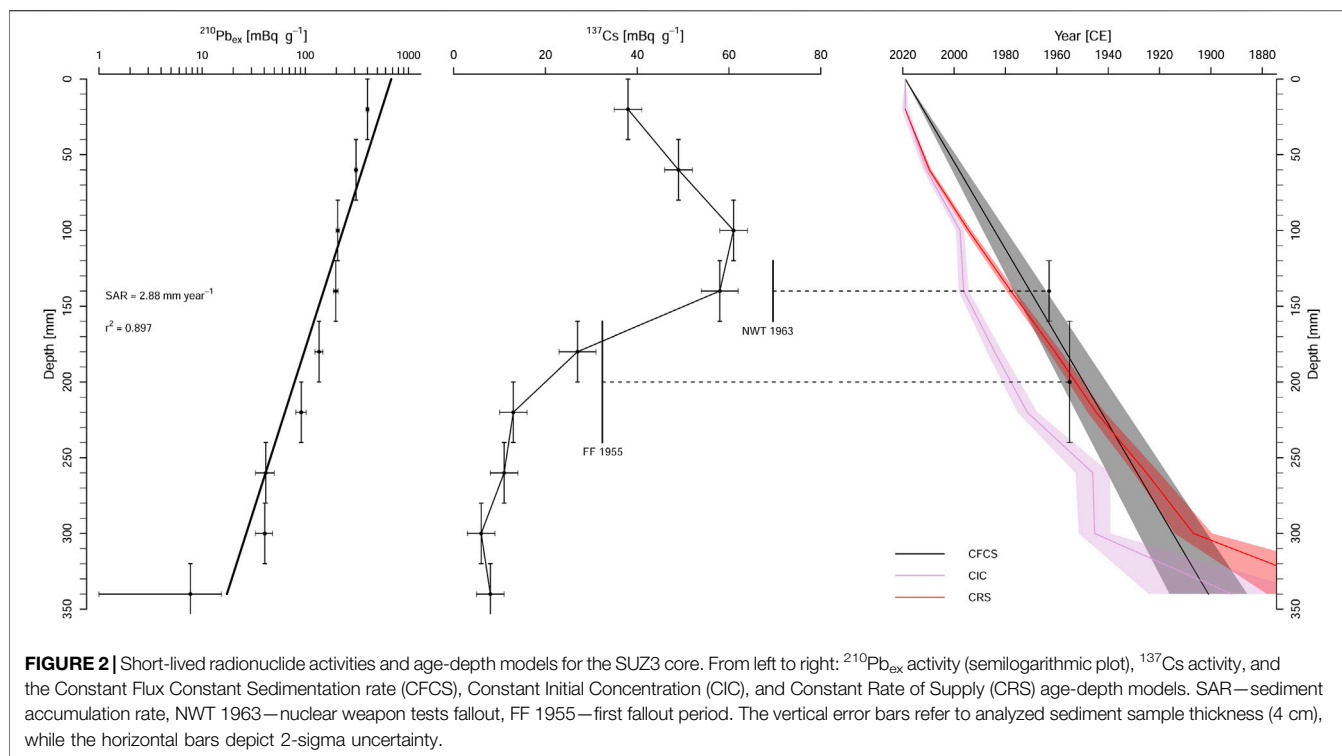
### 3.6 Diatoms and Freshwater Fauna Remains

Diatom analysis and the analysis of freshwater fauna remains were conducted at 1 cm resolution throughout the SUZ1 sediment core. Diatom samples were prepared following the method described by van der Werff (1955). The material was cleaned by adding 37% H<sub>2</sub>O<sub>2</sub> and heating to 80°C for about 1 h, then by the addition of KMnO<sub>4</sub>. Following digestion and centrifugation, the resulting clean material was diluted with distilled water to avoid excessive concentrations of diatom valves, which may hinder

reliable observations. Known quantities of *Lycopodium* spores were added to estimate diatom concentrations. Cleaned diatom valves were mounted in Naphrax<sup>®</sup>, a high-refractive index medium. In each sample, 400 diatom valves were identified and enumerated on random transects at 1,000× magnification (oil-immersion), using an Olympus BX53 microscope equipped with Differential Interference Contrast (Nomarski) optics and an Olympus UC30 Imaging System. Diatoms were categorized into five ecological groups according to their life form (modified according to Buczkó et al., 2013): 1) aerophyton (living in subaerial and terrestrial habitats), 2) benthos (living at the bottom and near shore, mainly in soft sediments), 3) periphyton (attached to submerged substrata or organisms; more sessile than benthic diatoms), 4) plankton (living in the water column), and 5) tychoplankton (taxa frequently encountered both in the water column and in surface sediments). In addition, the category of benthos was further subdivided into three subcategories: epipsamon (living attached to sand grains), benthos sensu stricto (lake benthos besides epipsamon), and river benthos. Furthermore, the D to C ratio of diatom valves to chrysophyte cysts was calculated. The chrysophyte cyst sums are expressed relative to the number of diatom frustules (two valves = one frustule) plus chrysophyte cysts, with the following formula: D:C = [number of diatom frustules/(number of chrysophyte cysts + number of diatom frustules)] × 100 (Douglas and Smol 1995).

Samples for zoological indicators were washed with distilled water through a 100 μm sieve and transferred into a modified plastic Sedgewick-Rafter counting cell. All identified animal remains, mainly chironomid (non-biting midge) head capsules (HCs), were picked with either fine forceps or a steel needle using a dissecting optical microscope (15× magnification). Samples were then dehydrated in ethyl alcohol (~96%) and mounted on glass microscope slides in Euparal<sup>®</sup> mounting medium. For taxa identification, we used an optical microscope (100–400× magnification) and followed several identification keys—mainly Wiederholm (1983), Rieradevall and Brooks (2001), Brooks et al. (2007), and Szeroczyńska and Sarmaja-Korjonen (2007). Due to low abundances of all zoological indicators, including chironomid HCs, in most of the samples, we show only concentrations of individual taxa (i.e., fossils per 1 g of dry sediment).

Statistically significant changes in the diatom record were determined using the optimum sum of squares partitioning on percentage data implementing the ZONE program (Birks and Gordon 1985; Lotter and Juggins 1991). The results from optimum sum of squares partitioning on percentage data were tested for significance using a broken-stick model to derive a stratigraphical zonation (Bennett 1996). Due to the presence of zero values in the chironomid record in some of the analyzed layers (which do not allow independent zonation), we use the diatom zonation when the zoological indicator data and other proxies are discussed.



## 4 RESULTS

### 4.1 Lake Bathymetry and Sediment Lithology

Figure 1C displays the morphobathymetric map of Suzdalevo Lake obtained after data processing and compilation, while **Supplementary Figure S2** shows echographic (depth) profiles with the depth magnified by a factor of 10. The lake is very shallow, with a maximum depth of about 2.3 m and a surface area of ~1.8 ha. The depth-to-diameter ratio is about 0.015, and its irregular inverted-cone morphology is slightly elongated in the N-S direction. The depocenter is located close to the N shore, while the E and W shores show morphological irregularities. Both sediment cores (SUZ1 and SUZ3) were recovered from the depocenter (**Figure 1C**) and consisted of homogeneous dark brown gyttja with no distinct lamination or a clayey layer.

### 4.2 Sediment Age Determination

In the SUZ1 core,  $^{210}\text{Pb}$ ,  $^{226}\text{Ra}$ , and  $^{137}\text{Cs}$  activities were measured only for the upper 26 cm. Due to their low values and large error bars (**Supplementary Figure S3**, **Supplementary Table S1**), the same measurements were not performed for the deeper layers. Excess (“unsupported”)  $^{210}\text{Pb}$  ( $^{210}\text{Pb}_{\text{ex}}$ ) was detected even in the deepest analyzed sample (depth of 25–26 cm), therefore the  $^{210}\text{Pb}_{\text{ex}}$  inventory could not be calculated. The  $^{137}\text{Cs}$  specific activities are relatively low and irregular at depths below 16 cm. The maximum  $^{137}\text{Cs}$  activity of  $93 \text{ Bq kg}^{-1}$  was detected at the depth of 9.5 cm. Weights of some SUZ1 samples were <1 g of dry sediment (average 0.9 g).

The problem of low sample weights in the SUZ1 core was resolved using the parallel core SUZ3, where four adjacent layers were merged to produce larger samples (3.1–5.6 g of dry sediment). In nine merged (4-cm-thick) layers, the specific activities of  $^{210}\text{Pb}$  decrease exponentially from the topmost layers to background (“supported”) activities in the lower part of the core, showing a relatively smooth decreasing curve (**Supplementary Figure S3**).  $^{210}\text{Pb}_{\text{ex}}$  was successfully detected in upper eight merged samples (**Figure 2**, **Supplementary Table S1**). The trend in the SUZ3 relation between  $^{210}\text{Pb}_{\text{ex}}$  and depth in core is similar to the SUZ1 record, but the curve is smoother and shows lower error bars (**Supplementary Figure S4**). The  $^{137}\text{Cs}$  specific activities are relatively low (maximum activity of  $61 \text{ Bq kg}^{-1}$ ), demonstrating low contamination by radioactive fallout. An increase in  $^{137}\text{Cs}$  activity, that should be equivalent with the global fallout due to nuclear weapon tests before its maximum in 1963 CE, was found between depths of 14 and 18 cm (**Figure 2**), with corresponding calculated ages of 1958–1963 years. CE (CRS model), 1988–1993 years. CE (CIC model), and 1963–1971 years. CE (CFCS model) for the average depth of 16 cm (**Supplementary Table S2**). However, this  $^{137}\text{Cs}$  peak is flat and low  $^{137}\text{Cs}$  activities are dispersed in all samples of the upper part of the core, probably due to continuous flushing out from the surrounding contaminated area, occasional sediment-water interface mixing (redeposition), and younger atmospheric fallout (later nuclear tests and power plant accidents).

Calculated sediment accumulation rates for the SUZ3 core differ among the age-depth models (**Supplementary Table S2**). Based on the CRS model, the accumulation rates decrease

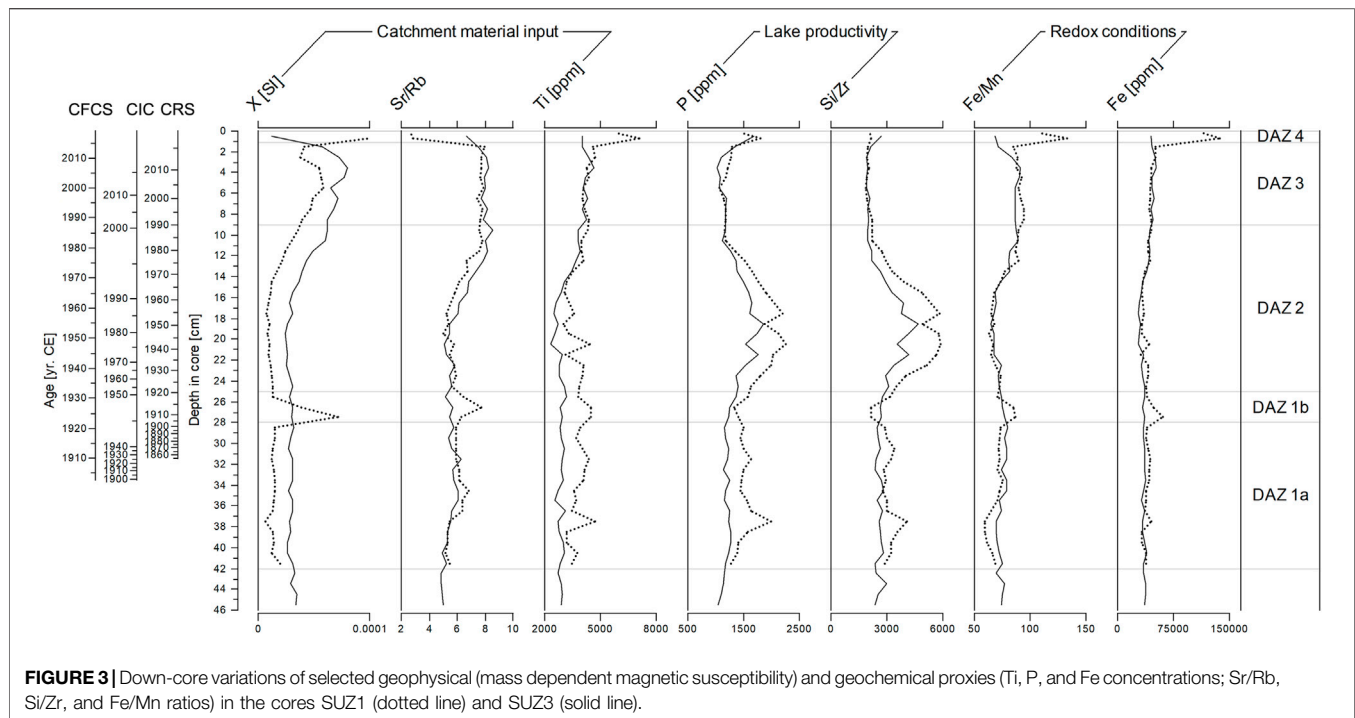


**FIGURE 3** | Down-core variations of selected geophysical (mass dependent magnetic susceptibility) and geochemical proxies (Ti, P, and Fe concentrations; Sr/Rb, Si/Zr, and Fe/Mn ratios) in the cores SUZ1 (dotted line) and SUZ3 (solid line).

downwards from 3.27 (depth of 4 cm) to 1.24 (depth of 32 cm)  $\text{mm year}^{-1}$ . The uppermost samples between 0 and 3 cm show intermediate accumulation rates increasing from 2.44 to 3.10  $\text{mm year}^{-1}$ . The CIC model shows two periods of high accumulation rate around 14 and 30 cm, and the CFCS model expects stable accumulation rate of 2.88  $\text{mm year}^{-1}$ . The age of 1908 CE (best fit) is placed to depths of 27.75, 32.84, and 32.00 cm according to the CRS, CIC, and CFCS models, respectively.

### 4.3 The Magnetic and Geochemical Record

Mass normalized magnetic susceptibility values [X (SI)] in the SUZ1 core show a peak at the depth of 27.5 cm and an increasing trend between the depths 15 and 0 cm (Figure 3). For the same core, the concentrations of selected elements (ppm) and their ratios are plotted with depth and the diatom zonation (see details in Section 3.5 and Figure 3) to better interpret the lake sedimentation history. Two proxies characterizing catchment material input to the lake are used. The Sr to Rb ratio has a similar trend as magnetic susceptibility (a peak at the depth of 26.5 cm and an increasing trend from 16 cm), except for a drop in the two uppermost layers that correspond to an increased concentration of Ti. Ti concentrations are otherwise relatively stable in the profile. Both proxies of primary productivity in the lake environment, P concentration and the Si to Zr ratio, show peaks at 37.5 cm, low values around 26.5 cm, and increased values between 24 and 12 cm (max. P concentration of  $\sim 2,250$  ppm and max. Si/Zr of  $\sim 5,800$ ) followed by low values (min. P concentration of  $\sim 1,070$  ppm and max. Si/Zr of  $\sim 1,850$ ). Trends of the Fe to Mn ratio curve correspond well with Fe concentrations, showing increased values around 27.5 cm and a sharp increase with maxima in the two uppermost layers (shifts from 85 to 133 for Fe/Mn and from  $\sim 50,500$  to  $\sim 137,200$  ppm for

the Fe concentration). The Fe to Mn ratio, a potential proxy for changes in the near-bottom redox conditions, was therefore determined by fluctuations in the Fe concentration.

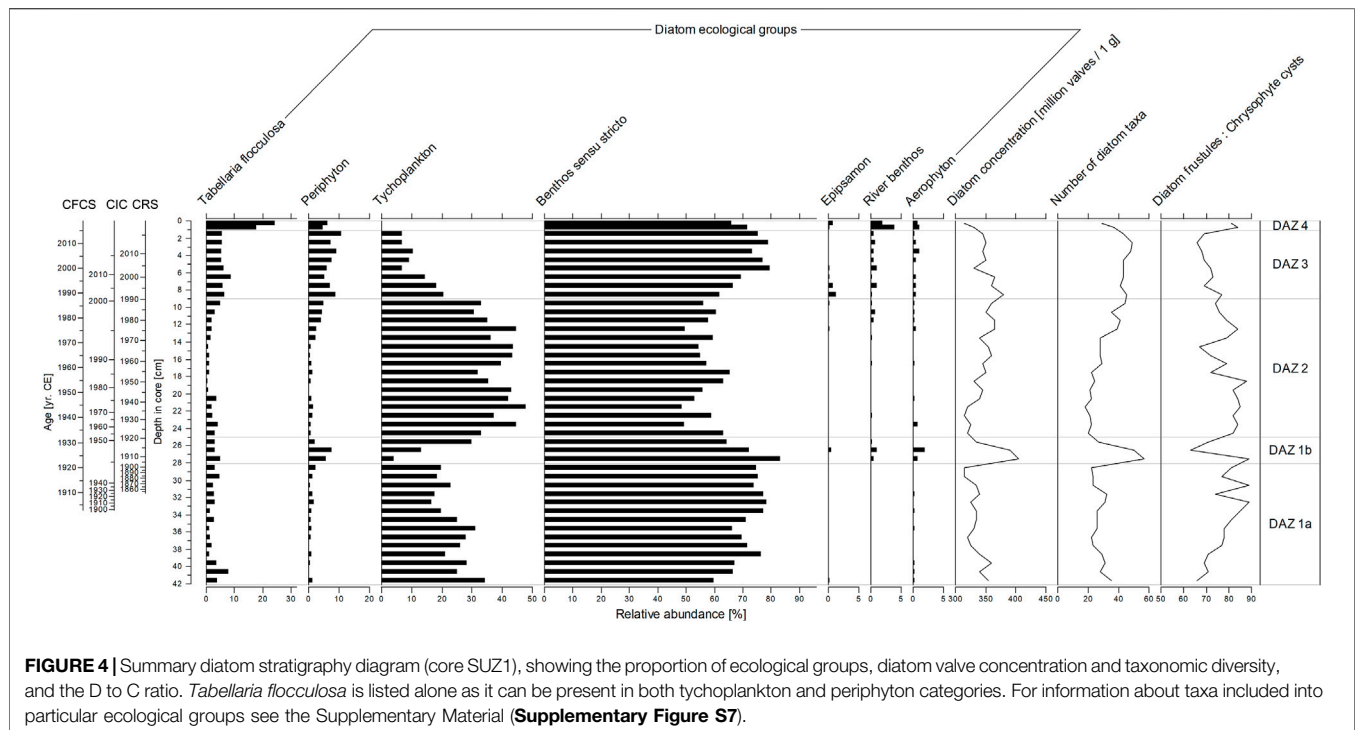
A similar magnetic susceptibility and geochemical record was found for the SUZ3 core (Figure 3). Nevertheless, it shows two noticeable differences: 1) absence of the magnetic susceptibility peak at the depth of 27.5 cm followed by the Sr/Rb peak at the depth of 26.5 cm, and 2) absence of the magnetic susceptibility, Ti, Fe/Mn, and Fe peaks in the two uppermost layers. Based on this comparison, the SUZ1 core provided more dynamic records and was selected for extraction of iron-rich microspherules and analyses of biological indicator remains.

### 4.4 Iron-Rich Microspherule Presence

During the SEM observation of the magnetic extract from the Suzdalevo Lake sediment, we found reduced (oxygen content  $< 50\%$ ) titanomagnetite (TM) grains in the depth interval of 26–30 cm (Supplementary Figure S5). However, their concentration is very low, not exceeding three grains per 1 g of dry sediment. Only one magnetic microspherule larger than 3  $\mu\text{m}$  in diameter was found in the same samples with an original wet volume of 28  $\text{cm}^3$  (14  $\text{cm}^3$  for the two youngest layers). This iron oxide microspherule (10  $\mu\text{m}$  in diameter; Fe 67.6%, O 30.4%, Cr  $< 1\%$ , Cu  $< 1\%$ ) was separated from the sample 3–4 cm ( $\sim 2011$  CE). Its outer surface exhibits a distinctive skeletal texture characteristic of rapid melting-quenching processes (Supplementary Figure S6).

### 4.5 Biological Indicators

Altogether, 156 diatom taxa representing 55 genera were identified in the sediment studied. The most abundant taxa include *Staurosira costruens* var. *venter* (Ehrenberg) P. B.



Hamilton, *Aulacoseira laevis* (Grunow) Krammer, *Pseudostauroneis brevistriata* (Grunow) D. M. Williams and Round, *Aulacoseira alpigera* (Grunow) Krammer, and *Tabellaria flocculosa* (Roth) Kützing (**Supplementary Figure S7**). Most of the taxa belong to benthos sensu stricto, tycho plankton, and periphyton, whereas the epipsamon, river benthos, and aerophyton ecological groups are rare (**Figure 4**). Although *Tabellaria flocculosa* is usually considered to be a planktonic diatom, periphytic forms can be also common. Therefore, we decided to keep this taxon as a separate category.

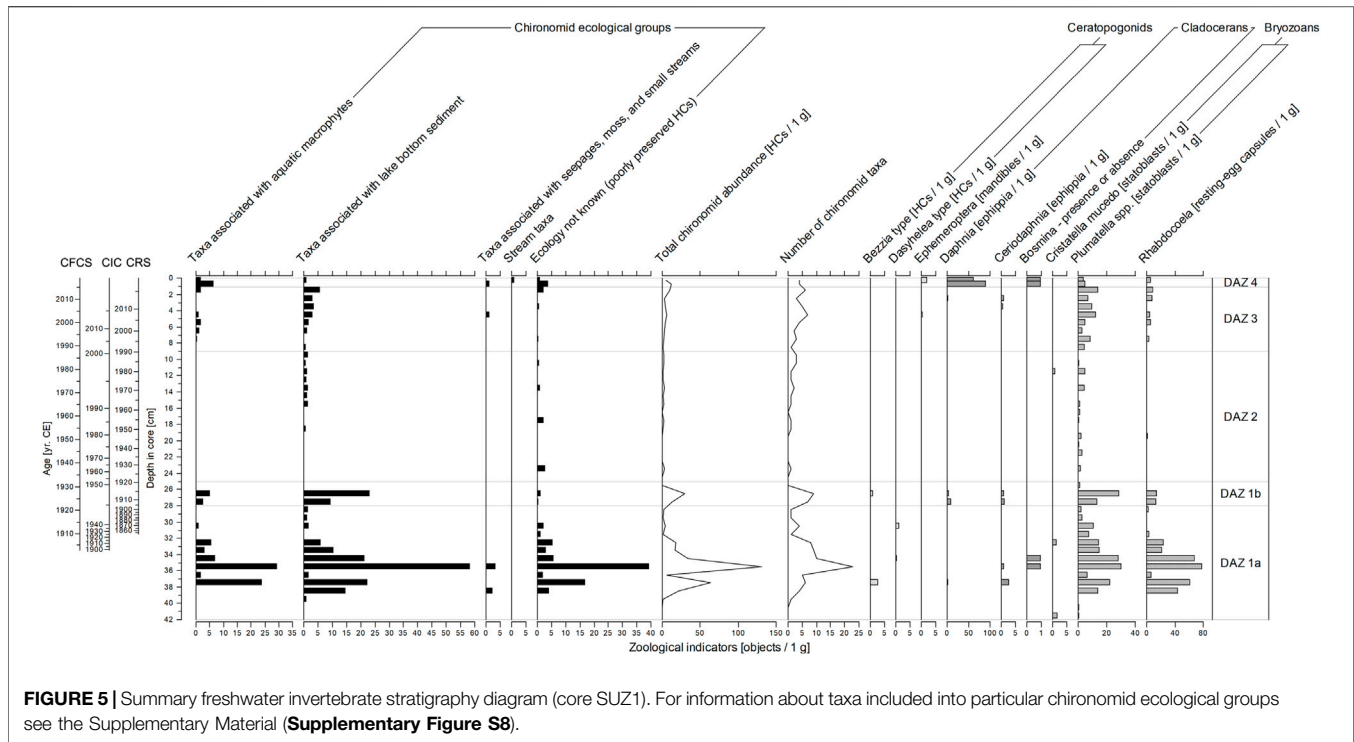
The diatom record was divided into four significant diatom assemblage zones (DAZ 1–4) based on the relative abundances. DAZ 1 was further divided into two subzones (DAZ 1a, DAZ 1b), because of striking changes in the diatom valve concentration per 1 g and diversity (number of species per 400 valves) at the depth of 28 cm (**Figure 4**).

The average concentration of chironomid head capsules (HCs) is 9.5 HCs per 1 g of dry sediment. While HCs in nine samples are absent, the maximum concentration of HCs in a single sample reaches 131 per 1 g of dry sediment. Altogether 33 chironomid taxa were identified (poorly preserved HCs identified to subfamily level were not counted). The most common components of the chironomid assemblages (at least 5 HCs per 1 g in one sample) are *Chironomus anthracinus*-type, *Cladotanytarsus mancus*-type, *Cricotopus intersectus*-type, *Dicrotendipes nervosus*-type, *Endochironomus impar*-type, *Psectrocladius sordidellus*-type, *Tanytarsus lugens*-type, and *T. mendax*-type (**Supplementary Figure S8**). In addition to chironomids (Diptera: Chironomidae), we also observed head capsules of biting midges (Diptera: Ceratopogonidae); mayfly (Ephemeroptera) mandibles; ephippia (genus *Ceriodaphnia* and

*Daphnia*), shells, and head shields (genus *Bosmina*) of planktonic cladocerans; bryozoan statoblasts (*Cristatella mucedo* and genus *Plumatella*); and microturbellarian (Turbellaria: Rhabdoceola) resting-egg capsules (**Figure 5**). However, these other zoological indicators are rather complementary to the chironomid record.

#### 4.5.1 DAZ 1a (42–28 cm)

This (sub)zone is characterized by high abundances of benthic and tycho planktonic diatom taxa, together with lower diversity and diatom valve concentration values. The zone is further characterized by fluctuation in the relative abundances of tycho planktonic *A. laevis* and *Aulacoseira italica* (Ehrenberg) Simonsen. Typical for those lowermost layers are high abundances of benthic colonial Fragilariaceae taxa including *S. construens* var. *venter* and *P. brevistriata*. Notable is the presence of acidophilous *Eunotia* species (*Eunotia glacialis* Meister, *Eunotia tenella* (Grunow) Hustedt or *Eunotia minor* (Kützing) Grunow) and a gradual increase in the D to C ratio. Chironomids, dominated by taxa associated with water macrophytes (e.g., *Dicrotendipes nervosus*-type and *Psectrocladius sordidellus*-type) and lake bottom sediment (*Chironomus anthracinus*-type and *Tanytarsus lugens*-type), reach their highest abundance and highest taxonomic diversity (number of taxa per samples), especially at the depth interval of 39–32 cm, peaking at 35.5 cm (131 HCs per 1 g of dry sediment). On the other hand, outside this depth interval, findings of chironomid HCs are rare (0–4 HCs per 1 g of dry sediment). The same trends were observed in abundances of bryozoan statoblasts and microturbellarian resting-egg capsules. Findings of ceratopogonid HCs and remains of planktonic cladocerans



(mainly *Bosmina*) are rare and occur in samples with increased abundances of chironomids.

#### 4.5.2 DAZ 1b (28–25 cm)

The onset of this (sub)zone is characterized by a sharp decrease of tychoplankton, whereas the abundances of benthos, periphyton and aerophyton increase markedly. Furthermore, remarkable changes in the diatom valve concentration and diversity occur in this section, with a significant peak of diversity and valve concentration at 27.5 cm, followed by a peak in chrysophyte cyst concentration (low D:C ratio) at 26.5 cm. The significant increase in periphyton is most apparent in the higher abundances of taxa indicative of greater habitat availability, such as *Cocconeis placentula* Ehrenberg, *Gomphonema parvulum* Kützing, and *Epithemia adnata* (Kützing) Brébisson. This zone is further characterized by the first occurrence of species of the genus *Psammothidium*, typically bound to sand grains (epipsamon), and river benthic taxa. In addition, several aerophilous diatoms, indicative of inwash from the lake catchment, such as *Hantzschia amphioxys* (Ehrenberg) Grunow, *Pinnularia borealis* Ehrenberg, and *Luticola acidoclinata* Lange-Bertalot are present. Chironomid abundance and taxonomic diversity as well as abundances of bryozoan statoblasts and microturbelarian resting-egg capsules reach the second highest peaks in DAZ 1b (up to 30 chironomid HCs per 1 g of dry sediment). The most dominant taxon, *Chironomus anthracinus*-type, is accompanied mainly by other eurytopic taxa living in bottom sediments (e.g., *Cladotanytarsus mancus*-type and *Microtendipes pedellus*-type). *Tanytarsus lugens*-type, an inhabitant of well-oxygenated cold lakes, is not present in the assemblages. Within the planktonic cladocerans, *Bosmina* is replaced by *Daphnia* and *Ceriodaphnia*.

In DAZ 1b, we also observed fine plant macroremains (length 1–5 mm) that were more abundant than in the other zones (**Supplementary Figure S9**).

#### 4.5.3 DAZ 2 (25–9 cm)

The relative abundances of tychoplanktonic taxa markedly increase (up to 48%), with a gradual increase of *A. laevis* from 15 to 33% at the onset of this zone, accompanied by a decrease in benthic taxa, diatom valve concentration, and diversity. Valve concentration and diversity are low at first, then rise gradually till the top of the zone. DAZ 2 is also characteristic by a rise and a subsequent steep decline in abundances of *A. italica*, and by extremely low abundances of chironomids HCs (0–3 HCs per 1 g of dry sediment). Chironomids associated with water macrophytes and remains of planktonic cladocerans disappear. In addition to bottom sediment associated chironomids, only bryozoan statoblasts of the genus *Plumatella* document the continuous presence of benthic invertebrates in DAZ 2.

#### 4.5.4 DAZ 3 (9–1 cm)

A marked decrease in the abundance of diatom tychoplankton occur at the base of this section and benthic *S. construens* var. *venter* become the most dominant taxon. A gradual decrease of tychoplanktonic *A. alpigena* and *A. laevis* is accompanied by a complete disappearance of *A. italica*. On the other hand, benthos, periphyton, aerophyton, and epipsamon increase, leading to relatively high taxonomic diversity of the assemblages. *Sellaphora saugerressi* (Desmazières) C.E.Wetzel and D.G.Mann, *Pseudostaurosira trainorii* E.A.Morales, *P. brevistriata*, and *Achnanthydium minutissimum* (Kützing)

Czarnecki form minor but characteristic elements of this zone, and the relative abundance of *Tabellaria flocculosa* increase markedly. Water macrophyte chironomids appear again, but total abundances of chironomid HCs increase only slightly (1–10 HCs per 1 g of dry sediment). This increase is more pronounced in bryozoan statoblasts and microturbelarian resting-egg capsules. The dominant chironomid taxa are similar to DAZ 1b—*Chironomus anthracinus*-type, *Dicrotendipes nervosus*-type, and *Microtendipes pedellus*-type; however, several *Tanytarsus lugens*-type specimens were also detected. Findings of *Daphnia* and *Ceriodaphnia ehippia* are rare and situated in the younger half of the zone. *Bosmina* remains are absent.

#### 4.5.5 DAZ 4 (1–0 cm)

A distinct shift in diatom assemblages occur in the two top layers of the core, showing a decrease in valve concentration and diversity with a simultaneous increase in chrysophyte cyst concentrations (high D:C ratio). The most prominent change in this zone is a gradual increase in abundances of *T. flocculosa* and a sudden disappearance of diatom tychoplankton, together with high abundances of river benthic (*Planothidium frequentissimum* (Lange-Bertalot) Lange-Bertalot) and aerophytic taxa (*Microcostatus krasskei* (Hustedt) J. R. Johansen and J. C. Sray, *H. amphioxys*). High abundances of *Aulacoseira* species are replaced by an increase in the abundance of species that inhabit shallow water environments. The benthic diatom *Staurosirella pinnata* (Ehrenberg) D. M. Williams and Round, first occurring in the lowermost layers of the core, suddenly becomes the dominant taxon. Apparent changes were also observed in the zoological indicators. The proportion of water macrophyte chironomids increases due to the first occurrence of *Endochironomus impar*-type in the assemblages, and a single finding of *Eukiefferiella claripennis*-type, a rheophilic taxa, was observed. However, chironomid abundances remain low, similarly to in DAZ 3 (5–12 HCs per 1 g of dry sediment). The taxonomic composition of planktonic cladocerans also changes, with ehippia of the genus *Ceriodaphnia* replaced by *Bosmina* remains and abundant ehippia of g. *Daphnia* (63–92 ehippia per 1 g of dry sediment).

## 5 DISCUSSION

### 5.1 The Origin of Suzdalevo Lake in Relation to the Tunguska Event

The cores SUZ1 and SUZ3 were collected at the same location within the Suzdalevo Lake basin and show relatively similar geochemical, magnetic, and short-lived isotope activity records (Figure 3, Supplementary Figure S3). Due to this similarity, although partial differences are apparent, we used the  $^{210}\text{Pb}$  dating of the SUZ3 core for interpretation of SUZ1 proxy data. In both cores, the observed peaks in  $^{137}\text{Cs}$  (onset of the peaks at the depth of ~16 cm; Figure 2, Supplementary Figure S4) were interpreted as signals of the global fallout from atmospheric nuclear weapons with the  $^{137}\text{Cs}$  maximum in 1963 CE (e.g., Appleby 2008; Bruel and Sabatier 2020),

including the tests carried out by the Soviet Union at Novaya Zemlya from 1957 to 1962 (Khalturin et al., 2004), which is in good agreement with the results of the CRS age-depth model (1958–1963 CE at the depth of 16 cm) for the SUZ3 core. This model is likely the most relevant one for dating of the younger half of the sedimentary record as it reflects well sediment compaction in middle parts of the cores. The signal of the Chernobyl accident in 1986, that was reported from many regions of the Northern Hemisphere, is not known from lake sediments investigated in the area of the TE (Rogozin et al., 2017; Darin et al., 2020). However, the maximum  $^{137}\text{Cs}$  peaks in Suzdalevo Lake cores are not very prominent. In SUZ1, low  $^{137}\text{Cs}$  activities were detectable also below the depth of 16 cm, likely due to partial mixing and/or remobilization and downward diffusion within the sediments (Matisoff 2017). Despite the fact that the “no sediment mixing” assumption for construction of the  $^{210}\text{Pb}$ -based age-depth models is not fully met, all three models (CRS, CIC, CFCS) show that the base samples of the studied sediment cores are older than 1908 CE (Figure 2, Supplementary Table S2). Since even the oldest layers contain valves of lake diatoms and remains of lake invertebrates, sedimentation in a lake environment is apparent throughout the whole record (Figures 4, 5). Moreover, the diatom and zoological indicator assemblages below the first layer with no  $^{210}\text{Pb}_{\text{ex}}$  activity (>36 cm, calculated ages >1908 CE) are not uniform (Figures 4, 5, Supplementary Figures S7, S8) which contradicts potential very high accumulation rate in a lake formed by the TE. Therefore, Suzdalevo Lake was evidently formed before the TE. Due to the nature of the studied material (short cores sampled by a gravity corer) it is not possible to determine the time or the process of lake formation. It can only be speculated that it may have been associated with the selective melting of permafrost that is still present in the region (Gasperini et al., 2007; Ponomarev et al., 2019). Despite the oral testimony of the Evenki people, Suzdalevo Lake is not a TE impact crater filled with water, as has been proposed for the basin of Cheko Lake (Collins et al., 2008; Rogozin et al., 2017). Note that this conclusion is supported by the depth to diameter ratio being lower than 1/100 (Figure 1C and Supplementary Figure S2), while typical simple impact craters have values between 1/5 and 1/7 (Melosh 1989; Włodarski et al., 2017).

On the other hand, the existence of the lake before the TE is not supported by identification of a specific “TE layer”. No distinct clayey TE layer was observed, in contrast to those documented in the sediments of Cheko Lake and Zapovednoe Lake (thickness from 2 to 8 mm) by Kletetschka et al. (2019a) and Darin et al. (2020), respectively (Supplementary Figure S10). This is probably due to the fact that Zapovednoe and Cheko lakes are deep riverine lakes with large catchments, while Suzdalevo is a small shallow water body separated from the Chamba River (Figure 1C, Supplementary Figures S1, S2). Sediments of riverine lakes and lakes with large tributaries are often very sensitive to erosion in a wider area compared to lakes with small catchments (e.g., Xu et al., 2010; Wilhelm et al., 2017). The most conspicuous, but not strong, clastic material input event in Suzdalevo Lake occurred in DAZ 4, based on the simultaneously increased values of mass normalized magnetic

susceptibility, the Sr to Rb ratio, and Ti concentration in the SUZ1 core (Rapuc et al., 2020). However, DAZ 4 represents the youngest part of the sedimentary record and no similar erosion signal was found in the SUZ3 core. Another evidence of disturbance to the lake catchment was observed between the depths 25 and 28 cm (DAZ 1b), i.e., 14 cm above the base of the SUZ1 core (**Figure 3**). The DAZ 1b (SUZ1 core) contains abundant fine plant remains (**Supplementary Figure S9**), and its onset is characterized by increases in mass normalized magnetic susceptibility and the Sr to Rb ratio. The mass normalized magnetic susceptibility values reflect the concentration of potential magnetic carriers in the sediment (magnetite, pyrrhotite, maghemite, titanomagnetite, titanomaghemite, greigite); therefore, their enhancement in DAZ 1b reflects the presence of higher concentrations of at least one of these carriers. Since the area was exposed to fires due to the explosion and extreme radiation from the sky (Svetsov 2002; Jenniskens et al., 2019; Johnston and Stern 2019), the burning of organic material (e.g., grass, herbs, tree leaves and branches) has been associated with the conversion of iron-bearing organic matter to magnetite (Kletetschka and Banerjee 1995). The increase in the Sr to Rb ratio also reflects the higher content of plant remains in the sediment samples rather than a decline in terrigenous clastic input (Xu et al., 2010). This is supported by the relatively stable Ti concentration values, indicating no distinct change in the proportion or grain size of clastic material (Cuven et al., 2010). The above mentioned geochemical and magnetic anomalies in DAZ 1b were, however, observed only in the SUZ1 core (**Figure 3**). The absence of similar shifts in the core SUZ3 implies variability of the disturbance signal strength within the lake basin. The DAZ 1b onset at the depth of 28 cm is in agreement with the CRS-model-calculated depth for 1908 CE (27.75 cm), however, this “TE-depth” is placed ca. 5 and 4.3 cm deeper according to the CIC and CFCS models, respectively. It is important to notice that the time of the TE (i.e., 111 years before the sediment coring) is close to the limit of the  $^{210}\text{Pb}$  dating method and the related models’ applicability. Moreover, when the CRS model is applied, a “too-old” age error is always present for the deeper core layers due to underestimation of  $^{210}\text{Pb}_{\text{ex}}$  (Binford 1990).

We found no increase in concentration of melted magnetic microspherules in layers of potential TE age. Possible existence of a layer containing these objects would have been used for validating the age-depth models. The lack of melted magnetic microspherules in the SUZ1 sediments means that the TE explosion produced less than 354 magnetic microspherules per  $1\text{ m}^2$ , assuming the diameter of our gravity corer. This agrees with the known maximum concentration of these objects near the TE epicenter (90 magnetic microspherules per  $1\text{ m}^2$ , when objects with diameter from 10 to several hundred  $\mu\text{m}$  were counted) as reported by Badyukov et al. (2011). They studied material collected in the early 1960s by an expedition led by K. P. Florenskii, and distinguished magnetic iron-oxide microspherules and magnetic silicate microspherules with metallic droplets, both subdivided based on the presence/absence of a Ni admixture. The single microspherule we found in the SUZ1 core (**Supplementary Figure S6**) corresponds to the

category of iron-rich spherules without a Ni admixture that was, according to Badyukov et al. (2011), likely created by a high-temperature process from terrestrial rocks (i.e., melted and evaporated due to sudden heat pulse, and later nucleated and/or quenched due to subsequent cooling). The same type of microspherules can be, however, of anthropogenic origin and transported for long distances if sufficiently small ( $<150\text{ }\mu\text{m}$  in diameter) (Zhang et al., 2011). The maximum calculated age of the extracted microspherule of 2003 CE (CFCS model, depth of 4 cm; **Supplementary Table S2**) indicates that it likely originated from the background micrometeorite flux, redeposition of an older TE sediment or soil, or anthropogenic activities. It seems that, due to their low concentration, these objects (diameter  $>3\text{ }\mu\text{m}$ ) cannot be effectively used as markers of the TE in lake sediment cores from the Tunguska region. Also, the somewhat reduced TM grains that were found at depths of 30–26 cm (**Supplementary Figure S5**) cannot be interpreted as clear evidence of the TE explosion. The concentration of these grains is low ( $<3$  grains per 1 g of dry sediment) and could have originated from the erosion of local volcanic rocks (Kamo et al., 2003). Such erosion in the lake catchment and subsequent inwash of the TM grains to the lake depocenter could have rather been associated with the TE-related forest disturbance. In future studies focused on lake sediments in the Tunguska region, the detection of increased concentrations of Ir and other Pt group elements may be more promising as follows from the “Northern” peat bog record presented by Hou et al. (2004).

## 5.2 Lake Ecosystem Changes at the Time of the Tunguska Event

In this study, we present the first diatom and freshwater zoological indicator records from the area exposed to the TE explosion in 1908 CE (**Figures 4, 5**). Throughout its recent history, Suzdalevo Lake lacked a significant planktonic diatom community and was dominated by tychoplanktonic *Aulacoseira* species together with small benthic alkaliphilic species of the Fragilariaceae family, commonly found in nutrient limited lakes with long periods of ice cover in alpine (Lotter et al., 1997; Karst-Riddoch et al., 2005), arctic (Douglas and Smol 1999; Laing and Smol 2000), and tundra regions (Westover et al., 2006). Similarly, the remains of planktonic cladocerans are rare in the sediments, demonstrating a greater suitability of the shallow lake habitats for benthic and littoral taxa (Szeroczyńska and Sarmaja-Korjonen 2007). This is supported by frequent findings of various benthic zoological indicators, such as chironomids, ceratopogonids, mayflies, bryozoans, or microturbellarians. All invertebrate taxa that were identified are known from the lakes in southern Siberia ( $42\text{--}65^\circ\text{N}$ ) or have a Holarctic distribution (e.g., Massard and Geimer 2008; Nazarova et al., 2008; Kotov 2016; Biskaborn et al., 2019).

According to the alternative age-depth models (**Figure 2, Supplementary Table S2**), the “TE-layer” and related signals of ecosystem changes should be located in DAZ 1a around the depth interval of 32–33 cm (CIC and CFCS models) or at the DAZ 1a/DAZ 1b transition, i.e., near the depth of 28 cm (CRS model). The first scenario is more likely in the case of the

underestimation sediment accumulation rate in deeper layers mentioned by Binford (1990), however, the second scenario is also realistic when considering the error bars and thickness of the sediment layers used for the dating (4 cm). Moreover, only the second scenario corresponds to a distinct abrupt shift in lake biota (Figures 4, 5). The reality of the first scenario would imply an absence of a unique signal in the diatom and zoological indicator records. Such a conclusion would, for example, be consistent to the observations from sediments of Lake Strzeszyńskie (W Poland) that experienced the Morasko iron meteorite shower 4.9–5.3 kyr.cal. BP (Pleskot et al., 2018). The estimated entry mass of the Morasko meteoroid was between 600 and 1,100 tons and fragments of this cosmic body formed seven impact craters with diameters ranging from 20 to 90 m (Bronikowska et al., 2017).

If the age of the DAZ 1b onset is ~1908 CE as suggested by the CRS model, the pre-TE status of Suzdalevo Lake is represented by the bottom zone (DAZ 1a) that is dominated by benthic colonial Fragilariaceae taxa (Figure 4, Supplementary Figure S7). These ecological generalists are common in lakes at high elevations and high latitudes, where ice-free intervals are short and nutrient supplies are low, although they also occur across a wide ecological gradient (Wolfe 2003). Furthermore, they inhabit the littoral zone, which is the first area to become ice-free (Westover et al., 2006). Thus, these taxa may quickly form blooms and outcompete larger diatoms during the short growing season (Smol 1988; Lotter et al., 1999; Grönlund and Kaupilla 2002). Fluctuations in abundances of all benthic zoological indicators (Figure 5 and Supplementary Figure S8) imply the alternating presence of at least one adverse factor. Such severe suppression of benthic fauna in lakes is often caused by oxygen depletion (hypoxia) or even anoxia (e.g., Moravcová et al., 2021). Also, the presence of *Ceriodaphnia ephippia* and *Plumatella* and *Cristatella mucedo* statoblasts indicates limiting near-bottom oxygen concentrations caused by the intensive decomposition of organic matter accompanied by pronounced thermal stratification, limiting oxygen replenishment (Ursenbacher et al., 2020). However, the stratification and oxygen depletion were not permanent, as documented by the high abundance and high taxonomic diversity of chironomid HCs at depths from 39 to 32 cm, where both taxa that are tolerant (e.g., *Chironomus anthracinus*-type) and sensitive (*Tanytarsus lugens*-type) to low oxygen concentrations (Brooks et al., 2007; Tichá et al., 2019) were observed. Short periods of more intense water column mixing (affecting the sediment-water interface) could have occurred during the recent lake history as suggested by detectable low  $^{137}\text{Cs}$  activities below the depth of 16 cm in both cores (Figure 2, Supplementary Figure S3), but such short-term changes cannot be reconstructed due to the time resolution of our records. The hypothesized changes in the mixing regime during DAZ 1a were likely triggered by an external factor, such as a climate change or a forest disturbance. A potential impact of floods is not supported by any erosion proxies (Figure 3) or presence of taxa indicative of running water environment (Figures 4, 5). Therefore, if a flood occurred, it did not have an erosive effect on the lake shore. Another possible explanation comes from the alternative age-depth models. If the “TE-depth”

calculation using CIC and CFCS models is more realistic than in the case of the CRS model, an effect of the TE explosion cannot be ruled out as well.

As mentioned above, the assemblages in DAZ 1b could represent a direct response of the lake-catchment ecosystem to the TE (Figures 4, 5). In diatoms, the occurrence of aerophyton indicates the influence of the substantial transport of terrestrial material from the lake catchment, whereas the high abundances of periphyton and benthos suggest greater substrate variability. These changes therefore correspond to the observed increase in the amount of fine plant remains and the peak in mass normalized magnetic susceptibility (SUZ1 core), documenting a disturbance of the surrounding taiga. Diatom assemblages are known to also be structured by organic matter content and/or availability (Grimes et al., 1980), which significantly increased during this period. The diversified conditions, together with the input of organic matter, most probably led to increased diatom diversity and valve concentration (Adrian et al., 1999). Our data do not imply any conditions promoting the growth of acidophilous taxa, possibly connected with acidification or acid rains, as previously suggested by Kolesnikov et al. (1998). This also applies to the diatom assemblages in DAZ 1a. However, the peak in diatom valve concentration in DAZ 1b could have been supported by mild eutrophication after the increased deposition of nitrogen (N), estimated by Kolesnikov et al. (2003) to 200,000 tons across the 2,000 km<sup>2</sup> of tree fall area. This extra N supply was interpreted as a result of the high-temperature oxidation of nitrogen in the atmosphere with formation of nitrogen oxides during the impact (Kolesnikov et al., 1998, 2003); however, it could also have arisen from another unconventional process. Boslough and Crawford (2008) modelled the TE explosion in the atmosphere and calculated an overpressure reaching 1 GPa at 6–8 km above the Earth's surface. Such a pressure wave allows the compression of N in air to reach near the liquid phase (Alkhaldi and Kroll 2019), and thus may have allowed the oxidation and creation of N species over the impacted area. The deposition value published by Kolesnikov et al. (2003) (1 ton per 1 ha) may be overestimated or apply only to sites located close to the TE epicenter (distance <10 km); however, even a smaller deposition could have affected Suzdalevo Lake, as by shown by Bergström and Jansson (2006). Moreover, an input of P-rich dust after the TE explosion-related thermal radiation and shockwave could be expected, transporting this key limiting nutrient to the studied lake and its catchment. No increase in P concentration was observed in the studied cores near the DAZ 1b onset or around the depth interval 32–32.84 cm (Figure 3), but trends in total P concentration sometimes differ from trends in biologically available P as shown by Norton et al. (2011). The taxonomic diversity and abundance of zoological indicators increase in DAZ 1b, with the dominance of *Chironomus anthracinus*-type and the absence of *Tanytarsus lugens*-type (Supplementary Figure S8) suggesting an improvement in near-bottom oxygen conditions but to a lesser extent than in the case of the period around the chironomid abundance and diversity peak at 35.5 cm (Johnson and Wiederholm 1989; Gąsiorowski and Sienkiewicz 2010). The potential destruction of the shoreline forest by the TE explosion could have caused increased wind speeds and

shortened the periods of thermal stratification *via* wind mixing of the water column, resulting in improved dissolved oxygen concentrations (Klaus et al., 2021). On the other hand, the concurrent inwash of organic material could have accelerated respiration and oxygen consumption rates, which had the opposite effect and prevented the reappearance of the sensitive *Tanytarsus lugens*-type (Luoto 2013). In any case, the observed changes in DAZ 1b do not indicate any major disturbance or lake ecosystem collapse.

After the DAZ 1b, the ecosystem did not return to the pre-TE state. A new equilibrium, represented by DAZ 2, was established, and lasted until the 1990s (i.e., ca. 50–70 years) (Figure 4). We interpret this zone as a period of low water transparency and pronounced oxygen depletion, indicated by the substantial increase in the tycho planktonic diatom taxa and extremely low abundances of all benthic zoological indicators, respectively. We assume that both processes were driven by the presence of additional dead plant biomass in the catchment after the TE. This led to a subsequent increase in dissolved organic carbon (DOC) production, and later to DOC leaching, DOC transport to the lake, and lake water brownification (Kopáček et al., 2018). The DOC leaching may have been amplified by reduced evapotranspiration in the disturbed forest, leading to increased soil moisture (Brothers et al., 2014; Kopáček et al., 2018). Brownification is a fundamental factor influencing lake ecosystem structure and function through more stable thermal stratification caused by increased absorption of solar radiation and limited light availability to benthic primary producers due to decreased water column transparency (Brothers et al., 2014; Solomon et al., 2015; Vasconcelos et al., 2016). These conditions likely caused the decline in benthic diatoms and especially in all benthic invertebrates, such as chironomids, ceratopogonids, bryozoans, and microturbellarians (Figures 4, 5). The chironomid abundances are so low in DAZ 2 (0–3 HCs per 1 g of dry sediment) that even episodic near-bottom anoxic conditions at the deepest part in the lake cannot be ruled out (Johnson and Wiederholm 1989; Houfková et al., 2017; Urtenbacher et al., 2020). These conditions would have supported *Aulacoseira* species (Supplementary Figure S7), which are adapted to low light availability (Kilham 1990; Bradbury et al., 1994), but most of them also indicate turbulent, unstable environments, likely caused by mixing of the water column. Such ecological characteristics are related to the production of heavy resting cells during the *Aulacoseira* life cycle that requires resuspension from the sediments into the lake water to establish (tycho) planktonic populations (Round et al., 1990). In addition, *Aulacoseira* species also create heavy silicified vegetative cells and therefore require an increased degree of turbulence to prevent their sedimentation (Saunders et al., 2009; Buczkó et al., 2013). In view of these facts, the stratification could not be long-term, but occurred frequently enough to disadvantage the benthic fauna. A similar record showing a long-term *Aulacoseira* presence in a shallow lake affected by anoxia was published by Houfková et al. (2017). We can speculate that a severe winter stratification due to long ice cover period was the key factor that suppressed the benthic invertebrates but enabled a summer bloom of *Aulacoseira*.

While the highest diatom valve concentration per 1 g of dry sediment was observed in DAZ 1b, the highest P concentrations and the highest values of the Si to Zr ratio, the other two potential proxies for algal primary production (e.g., Cuven et al., 2011), were observed in DAZ 2 (Figure 3). We explain this discrepancy by the above-mentioned presence of large and heavy silicified *Aulacoseira* valves in DAZ 2, which could have increased the total diatom biomass and the concentration of biogenic silica (i.e., the Si to Zr ratio) in the sediment samples. Alternatively, the increased P content in DAZ 2 could be explained by an increase in P immobilization in the sediments caused by a higher aluminum hydroxide to iron hydroxide ratio in highly organic sediments during the brownwater phase, as shown by Kopáček et al. (2007). In the latter case, P concentration values would not reflect the availability of this limiting nutrient for aquatic organisms.

Since about the 1990s (DAZ 3), the lake biota in Suzdalevo Lake began to resemble those of the DAZ 1a (Figures 4, 5). The overall dominance of benthic diatoms (around 70% of the total diatom assemblage) may be attributed to processes linked to increased water transparency and with more stable conditions after recovery of the taiga forest, when DOC concentration in the lake water decreased and mature trees on the lake shore started to attenuate water mixing by wind (Kilham, 1990; Westover et al., 2006). The higher diatom diversity could be explained by the decreased dominance of *Aulacoseira* taxa, leading to more even diatom communities. These new conditions were also more favorable for benthic invertebrates, including taxa associated with aquatic macrophytes, that were absent in DAZ 2.

We also attempted to document changes in oxygen availability and related redox conditions in the sedimentary record using the Fe to Mn ratio (Figure 3). This proxy is based on the fact that Mn is more easily mobilized and passes into solution more readily than Fe under reducing conditions (Davison, 1993). However, in Suzdalevo Lake, trends in the Fe to Mn ratio coincide with the Fe concentrations, indicating that the ratio was mainly affected by changes in Fe supply from the lake catchment (Mackereth 1966), and thus could not be used to reconstruct changes in redox conditions.

### 5.3 Recent Environmental Changes in the Suzdalevo Lake Sedimentary Record

The SUZ1 core provided an anomalous multi-proxy record for the uppermost two layers (DAZ 4), representing approximately the years 2016–2019 CE. In spite of the absence of these anomalies in the SUZ3 core that indicates variability of the signal strength within the lake basin or partial loss of the surface layer during the coring, the shifts observed in most of the proxies in the SUZ1 core are conspicuous and deserve a separate comment (Figure 3). The low Sr to Rb ratio and the sharp increase in Ti concentrations in DAZ 4 document an increased input of clastic material (Cuven et al., 2010; Xu et al., 2010), which was not observed in the other zones, including the depth interval where “TE-depth” is expected according to the age-depth models. Such a change in the proportion of inorganic particles could have been caused by

increased erosion in the catchment or by flood activity of the nearby Chamba River (**Supplementary Figure S1**). Also, river benthic diatom taxa, such as *P. frequentissimum* (**Figure 4**, **Supplementary Figure S7**), reach their maximum abundance in DAZ 4, indicating a possible riverine influx and, together with higher abundances of aerophyton, may reflect the increased input of allochthonous material. In addition, the low diatom diversity and valve concentration and the dominance of *S. pinnata* and *T. flocculosa* suggest the persistence of relatively unproductive conditions throughout this period (Dam et al., 1994; Hofmann et al., 2011).

The same zone is characterized by the presence of abundant remains of two planktonic cladocerans, *Daphnia* and *Bosmina*, while the abundances of the benthic zoological indicators remain rather low (**Figure 5**). Among these benthic invertebrates, the only exception is the slight increase in chironomids associated with aquatic macrophytes and the solitary finding of the rheophilic chironomid *Eukiefferiella claripennis*-type (Brooks et al., 2007) (**Supplementary Figure S8**). Thus, the zoological record also suggests the influence of an external factor that changed conditions in the lake. DOC concentrations in boreal streams are often the lowest after high discharge events arising from snowmelt (e.g., Jonsson et al., 2007). If the factor responsible for the observed changes in lake biota was a snowmelt flood (or several floods during the period 2016–2019 CE) on the Chamba River, a drop in DOC accompanied with an increase in water transparency, along with other changes in water chemistry, could have occurred in Suzdalevo Lake. Such a shift would, for example, support the growth of aquatic plants and increase the abundances of the associated chironomid taxa (**Figure 5**). Due to the presence of *Bosmina*, a cladoceran well adapted to fish predation, short-time colonization of the lake by fish after a flood event cannot be ruled out either (Johnsen and Raddum 1987); however, we did not observe any fish during our field survey.

We do not have data on floods on the Chamba River and we do not know of any observations of changes in the connectivity between Suzdalevo Lake and the river, as the site is very remote. Nevertheless, based on available data from the nearest meteorological station in Vanavara (Weather and Climate 2021), severe floods caused by rapid snowmelt or an ice jam near the study site could have occurred during the given period. At this station, the average annual temperature and precipitation between the years 1933 and 2020 were  $-5.5^{\circ}\text{C}$  and 421 mm, respectively, while between the years 2016 and 2019 the average annual temperature increased to  $-4.1^{\circ}\text{C}$  and average annual precipitation increased to 625 mm. This change in the local climate would have been favorable for stronger snowmelt floods and corresponds to trends observed in the wider area of Central Siberia (e.g., Tchebakova et al., 2011).

## 6 CONCLUSION

The TE in 1908 CE was an unusual extreme event that became part of the Evenki oral heritage. We performed this study to assess the potential for a TE-related origin of Suzdalevo Lake, a shallow water body located in the TE tree fall area, and to understand the

effects of the catastrophic explosion on the lake-catchment ecosystem. Our data show that the lake basin did not originate from the impact, but lake sediments from the site provide a multi-proxy record of a disturbance that occurred within a 5-cm-thick depth interval calculated using three alternative age-depth models for the position of the year 1908 CE. However, a clear link between this disturbance and the TE was not proven as the Suzdalevo Lake sediments do not contain an erosional clayey TE-layer, that was observed in the Zapovednoe and Cheko riverine lakes, or any melted magnetic microspherules produced by the TE explosion. We interpret the observed abrupt changes in the proxy records as the consequences of the inwash of dead plant biomass to the lake, increased wind mixing of the water column possibly caused by deforestation of the shoreline, and mild eutrophication by elevated nutrient input. After the phase of higher productivity (i.e., increased concentrations and taxonomic diversity of diatom valves and zoological indicator remains), the lake did not return to its original state for about 50–70 years, likely due to the increased DOC supply from its catchment and associated truncation of the photic zone and near-bottom hypoxia. Such changes in a lake environment that may be related to the TE are reported here for the first time, however, more lakes in the TE tree fall area should be studied to reveal the real impact of the TE on ecosystems.

## DATA AVAILABILITY STATEMENT

The datasets presented in this study can be found in the **Supplementary Material** and the PANGAEA online repository. The accession link can be found in the **Supplementary Material**.

## AUTHOR CONTRIBUTIONS

DV, RK and GK designed the research. RK, GK, MT and CS organized and performed the coring and morphobathymetric measurements. RK, DV, VG, ES, BC and RŠ performed the lab research. RK, DV, BC, VG, CS and GK analyzed the data. DV, RK, BC, and GK wrote the paper with final contributions from ES, MT, VG, RŠ and CS.

## FUNDING

Financial support for the research was provided by the Czech Science Foundation (Project No. 20-08294S—PROGRESS) and the Ministry of Education Youth and Sports of the Czech Republic (Project No. LTAUSA19141—PAGEO).

## ACKNOWLEDGMENTS

The authors would like to thank Evgenia Karnouchova, Leonid Krivobokov, Artur V. Meydus, Liudmila Mukhortova, and other workers of the Tunguska State Reserve for helping us in planning

and ensuring the smooth running of the entire expedition, Nicholas Hasson for help during the coring, Evžen Stuchlík for helpful comments on interpretation of our results, Petra Pokorná for help with R software, and David Hardekopf for language corrections. We also thank both reviewers for improving the manuscript *via* their comments.

## REFERENCES

Adrian, R., Walz, N., Hintze, T., Hoeg, S., and Rusche, R. (1999). Effects of Ice Duration on Plankton Succession during spring in a Shallow Polymictic Lake. *Freshw. Biol.* 41 (3), 621–634. doi:10.1046/j.1365-2427.1999.00411.x

Alkhaldi, H., and Kroll, P. (2019). Chemical Potential of Nitrogen at High Pressure and High Temperature: Application to Nitrogen and Nitrogen-Rich Phase Diagram Calculations. *J. Phys. Chem. C* 123, 7054–7060. doi:10.1021/acs.jpcc.9b00476

Appleby, P. G. (2008). Three Decades of Dating Recent Sediments by Fallout Radionuclides: a Review. *The Holocene*. 18 (1), 83–93. doi:10.1177/0959683607085598

Artemieva, N. A., and Shuvalov, V. V. (2016). From Tunguska to Chelyabinsk via Jupiter. *Annu. Rev. Earth Planet. Sci.* 44, 37–56. doi:10.1146/annurev-earth-060115-012218

Badyukov, D. D., Ivanov, A. V., Raitala, J., and Khisina, N. R. (2011). Spherules from the Tunguska Event Site: Could They Originate from the Tunguska Cosmic Body? *Geochem. Int.* 49 (7), 641–653. doi:10.1134/S0016702911070032

Bennett, K. D. (1996). Determination of the Number of Zones in a Biostratigraphical Sequence. *New Phytol.* 132, 155–170. doi:10.1111/j.1469-8137.1996.tb04521.x

Bergström, A.-K., and Jansson, M. (2006). Atmospheric Nitrogen Deposition Has Caused Nitrogen Enrichment and Eutrophication of Lakes in the Northern Hemisphere. *Glob. Change Biol.* 12, 635–643. doi:10.1111/j.1365-2486.2006.01129.x

Binford, M. (1990). Calculation and Uncertainty Analysis of 210Pb Dates for PIRLA Project lake Sediment Cores. *J. Paleolimnol.* 3, 253–267. doi:10.1007/BF00219461

Birks, H. J. B., and Gordon, A. D. (1985). *Numerical Methods in Quaternary Pollen Analysis*. London: Academic Press.

Biskaborn, B. K., Nazarova, L., Pstryakova, L. A., Syrykh, L., Funck, K., Meyer, H., et al. (2019). Spatial Distribution of Environmental Indicators in Surface Sediments of Lake Bolshoe Toko, Yakutia, Russia. *Biogeosciences*. 16, 4023–4049. doi:10.5194/bg-16-4023-2019

Bonatti, E., Breger, D., Di Rocco, T., Franchi, F., Gasperini, L., Polonia, A., et al. (2015). Origin of John's Stone: A Quartzitic boulder from the Site of the 1908 Tunguska (Siberia) Explosion. *Icarus*. 258, 297–308. doi:10.1016/j.icarus.2015.06.018

Boslough, M. B. E., and Crawford, D. A. (2008). Low-altitude Airbursts and the Impact Threat. *Int. J. Impact Eng.* 35, 1441–1448. doi:10.1016/j.ijimpeng.2008.07.053

Bradbury, J. P., Bezrukova, Y. V., Chernyaeva, G. P., Colman, S. M., Khursevich, G., King, J. W., et al. (1994). A Synthesis of post-glacial Diatom Records from Lake Baikal. *J. Paleolimnol.* 10 (3), 213–252. doi:10.1007/BF00684034

Bronikowska, M., Artemieva, N. A., and Wünnemann, K. (2017). Reconstruction of the Morasko Meteoroid Impact-Insight from Numerical Modeling. *Meteorit. Planet. Sci.* 52 (8), 1704–1721. doi:10.1111/maps.12882

Brooks, S. J., Langdon, P. G., and Heiri, O. (2007). *The Identification and Use of Palaeoarctic Chironomidae Larvae in Palaeoecology. QRA Technical Guide No. 10*. London: Quaternary Research Association.

Brothers, S., Köhler, J., Attermeyer, K., Grossart, H. P., Mehner, T., Meyer, N., et al. (2014). A Feedback Loop Links Brownification and Anoxia in a Temperate, Shallow lake. *Limnol. Oceanogr.* 59, 1388–1398. doi:10.4319/lo.2014.59.4.1388

Brown, P. G., Assink, J. D., Astiz, L., Blaauw, R., Boslough, M. B., Borovička, J., et al. (2013). A 500-kiloton Airburst over Chelyabinsk and an Enhanced hazard from Small Impactors. *Nature*. 503 (7475), 238–241. doi:10.1038/nature12741

## SUPPLEMENTARY MATERIAL

The Supplementary Material for this article can be found online at: <https://www.frontiersin.org/articles/10.3389/feart.2022.777631/full#supplementary-material>

Bruel, R., and Sabatier, P. (2020). *Serac*: an R Package for Shortlived RADionuclide Chronology of Recent Sediment Cores. *J. Environ. Radioactivity*. 225, 106449. doi:10.1016/j.jenvrad.2020.106449

Buczko, K., Magyari, E. K., Braun, M., and Bálint, M. (2013). Diatom-inferred Lateglacial and Holocene Climatic Variability in the South Carpathian Mountains (Romania). *Quat. Int.* 293, 123–135. doi:10.1016/j.quaint.2012.04.042

Collins, G. S., Artemieva, N., Wünnemann, K., Bland, P. A., Reimold, W. U., and Koerber, C. (2008). Evidence that Lake Cheko Is Not an Impact Crater. *Terra Nova*. 20, 165–168. doi:10.1111/j.1365-3121.2008.00791.x

Covey, C., Thompson, S. L., Weissman, P. R., and MacCracken, M. C. (1994). Global Climatic Effects of Atmospheric Dust from an Asteroid or Comet Impact on Earth. *Glob. Planet. Change*. 9 (3–4), 263–273. doi:10.1016/0921-8181(94)90020-5

Cuven, S., Francus, P., and Lamoureux, S. F. (2010). Estimation of Grain Size Variability with Micro X-ray Fluorescence in Laminated Lacustrine Sediments, Cape Bounty, Canadian High Arctic. *J. Paleolimnol.* 44, 803–817. doi:10.1007/s10933-010-9453-1

Cuven, S., Francus, P., and Lamoureux, S. (2011). Mid to Late Holocene Hydroclimatic and Geochemical Records from the Varved Sediments of East Lake, Cape Bounty, Canadian High Arctic. *Quat. Sci. Rev.* 30, 2651–2665. doi:10.1016/j.quascirev.2011.05.019

Dam, H., Mertens, A., and Sinkeldam, J. (1994). A Coded Checklist and Ecological Indicator Values of Freshwater Diatoms from the Netherlands. *Neth. J. Aquat. Ecol.* 28 (1), 117–133. doi:10.1007/BF02334251

Darin, A. V., Rogozin, D. Y., Meydus, A. V., Babich, V. V., Kalugin, I. A., Markovich, T. I., et al. (2020). Traces of the Tunguska Event (1908) in Sediments of Zapovednoe Lake Based on SR-XRF Data. *Dokl. Earth Sc.* 492 (2), 442–445. doi:10.1134/S1028334X20060045

Davison, W. (1993). Iron and Manganese in Lakes. *Earth-Science Rev.* 34, 119–163. doi:10.1016/0012-8252(93)90029-7

Douglas, M. S. V., and Smol, J. P. (1999). “Freshwater Diatoms as Indicators of Environmental Change in the High Arctic,” in *The Diatoms: Applications for the Environmental and Earth Sciences*. Editors E. F. Stoermer and J. P. Smol (Cambridge: Cambridge University Press), 227–244.

Douglas, M. S. V., and Smol, J. P. (1995). Paleolimnological Significance of Observed Distribution Patterns of Chrysophyte Cysts in Arctic Pond Environments. *J. Paleolimnol.* 13 (1), 79–83. doi:10.1007/BF00678112

Foschini, L., Gasperini, L., Stanghellini, C., Serra, R., Polonia, A., and Stanghellini, G. (2019). The Atmospheric Fragmentation of the 1908 Tunguska Cosmic Body: Reconsidering the Possibility of a Ground Impact. arXiv: Earth and Planetary Astrophysics, 1810.07427. <https://ui.adsabs.harvard.edu/abs/2018arXiv181007427F/abstract>

Froggatt, C. D., and Nielsen, H. B. (2015). Tunguska Dark Matter ball. *Int. J. Mod. Phys. A* 30 (13), 1550066. doi:10.1142/S0217751X15500669

Gąsiorowski, M., and Sienkiewicz, E. (2010). The Little Ice Age Recorded in Sediments of a Small Dystrophic mountain lake in Southern Poland. *J. Paleolimnol.* 43 (3), 475–487. doi:10.1007/s10933-009-9344-5

Gasperini, L., Alvisi, F., Biasini, G., Bonatti, E., Longo, G., Pipan, M., et al. (2007). A Possible Impact Crater for the 1908 Tunguska Event. *Terra Nova*. 19 (4), 245–251. doi:10.1111/j.1365-3121.2007.00742.x

Gasperini, L., Bonatti, E., Albertazzi, S., Forlani, L., Accorsi, C. A., Longo, G., et al. (2009). Sediments from Lake Cheko (Siberia), a Possible Impact Crater for the 1908 Tunguska Event. *Terra Nova*. 21, 489–494. doi:10.1111/j.1365-3121.2009.00906.x

Gasperini, L. (2015). Lake Cheko and the 1908 Tunguska Event. *Rend. Fis. Acc. Lincei*. 26, 97–108. doi:10.1007/s12210-015-0403-8

Gasperini, L., Stanghellini, C., and Serra, R. (2014). The Origin of Lake Cheko and the 1908 Tunguska Event Recorded by forest Trees. *Terra Nova*. 26 (6), 440–447. doi:10.1111/ter.12118

- Gasparini, L., and Stanghellini, G. (2009). SeisPrho: An Interactive Computer Program for Processing and Interpretation of High-Resolution Seismic Reflection Profiles. *Comput. Geosciences*. 35 (7), 1497–1507. doi:10.1016/j.cageo.2008.04.014
- German, B. R. (2019). *Crisis of the Meteorite Paradigm: Craters, Tektites, the Tunguska Event*. Freiburg: Freiburg Verlag.
- Gladkochub, D., Pisarevsky, S., Donskaya, T., Natapov, L., Mazukabzov, A., Stanevich, A., et al. (2006). The Siberian Craton and its Evolution in Terms of the Rodinia Hypothesis. *Episodes*. 29 (3), 169–174. doi:10.18814/epiuiugs/2006/v29i3/002
- Gladysheva, O. G. (2012). Atmospheric Anomalies in the Summer of 1908: Skyglow. *Geomagn. Aeron.* 52 (4), 526–532. doi:10.1134/S001679321203005X
- Gladysheva, O. (2020a). Swarm of Fragments from the Tunguska Event. *Mon. Not. R. Astron. Soc.* 496, 1144–1148. doi:10.1093/mnras/staa1620
- Gladysheva, O. (2020b). The Tunguska Event. *Icarus*. 348, 113837. doi:10.1016/j.icarus.2020.113837
- Grimes, J. A., Clair, St. L. L., and Rushforth, S. R. (1980). A Comparison of Epiphytic Diatom Assemblages on Living and Dead Stems of the Common Grass *Phragmites Australis*. *Great Basin Nat.* 40 (3), 223–228.
- Grönlund, T., and Kauppila, T. (2002). Holocene History of Lake Soldatskoje (Kola Peninsula, Russia) Inferred from Sedimentary Diatom Assemblages. *Boreas*. 31, 273–284. doi:10.1080/030094802760260382
- Hamrová, E., Goliáš, V., and Petrusek, A. (2010). Identifying century-old Long-Spined Daphnia: Species Replacement in a mountain lake Characterised by Paleogenetic Methods. *Hydrobiologia*. 643 (1), 97–106. doi:10.1007/s10750-010-0127-9
- Hofmann, G., Werum, M., and Lange-Bertalot, H. (2011). *Diatomeen im Süßwasser-Benthos von Mitteleuropa: Bestimmungsfloren Kieselalgen für die ökologische Praxis; über 700 der häufigsten Arten und ihrer Ökologie*. Rugell: A.R.G. Gantner.
- Hou, Q. L., Kolesnikov, E. M., Xie, L. W., Kolesnikova, N. V., Zhou, M. F., and Sun, M. (2004). Platinum Group Element Abundances in a Peat Layer Associated with the Tunguska Event, Further Evidence for a Cosmic Origin. *Planet. Space Sci.* 52 (4), 331–340. doi:10.1016/j.pss.2003.08.002
- Houfková, P., Bešta, T., Bernardová, A., Vondrák, D., Pokorný, P., and Novák, J. (2017). Holocene Climatic Events Linked to Environmental Changes at Lake Komořany Basin, Czech Republic. *The Holocene*. 27 (8), 1132–1145. doi:10.1177/0959683616683250
- Israde-Alcántara, I., Bischoff, J. L., Dominguez-Vázquez, G., Li, H.-C., DeCarli, P. S., Bunch, T. E., et al. (2012). Evidence from central Mexico Supporting the Younger Dryas Extraterrestrial Impact Hypothesis. *Proc. Natl. Acad. Sci. U.S.A.* 109 (13), E738–E747. doi:10.1073/pnas.1110614109
- Jenniskens, P., Popova, O. P., Glazachev, D. O., Podobnaya, E. D., and Kartashova, A. P. (2019). Tunguska Eyewitness Accounts, Injuries, and Casualties. *Icarus*. 327, 4–18. doi:10.1016/j.icarus.2019.01.001
- Johnsen, G. H., and Raddum, G. G. (1987). A Morphological Study of Two Populations of *Bosmina Longispina* Exposed to Different Predation. *J. Plankton Res.* 9 (2), 297–304. doi:10.1093/plankt/9.2.297
- Johnson, R. K., and Wiederholm, T. (1989). Classification and Ordination of Profundal Macroinvertebrate Communities in Nutrient Poor, Oligo-Mesohumic Lakes in Relation to Environmental Data. *Freshw. Biol.* 21 (3), 375–386. doi:10.1111/j.1365-2427.1989.tb01370.x
- Johnston, C. O., and Stern, E. C. (2019). A Model for thermal Radiation from the Tunguska Airburst. *Icarus*. 327, 48–59. doi:10.1016/j.icarus.2019.01.028
- Jonsson, A., Ström, L., and Åberg, J. (2007). Composition and Variations in the Occurrence of Dissolved Free Simple Organic Compounds of an Unproductive lake Ecosystem in Northern Sweden. *Biogeochemistry*. 82, 153–163. doi:10.1007/s10533-006-9060-4
- Kamo, S. L., Czamanske, G. K., Amelin, Y., Fedorenko, V. A., Davis, D. W., and Trofimov, V. R. (2003). Rapid Eruption of Siberian Flood-Volcanic Rocks and Evidence for Coincidence with the Permian-Triassic Boundary and Mass Extinction at 251 Ma. *Earth Planet. Sci. Lett.* 214, 75–91. doi:10.1016/S0012-821X(03)00347-9
- Karst-Riddoch, T. L., Pisaric, M. F. J., and Smol, J. P. (2005). Diatom Responses to 20th century Climate-Related Environmental Changes in High-Elevation mountain lakes of the Northern Canadian Cordillera. *J. Paleolimnol.* 33, 265–282. doi:10.1007/s10933-004-5334-9
- Kartashova, A. P., Popova, O. P., Glazachev, D. O., Jenniskens, P., Emel'yanenko, V. V., Podobnaya, E. D., et al. (2018). Study of Injuries from the Chelyabinsk Airburst Event. *Planet. Space Sci.* 160, 107–114. doi:10.1016/j.pss.2018.04.019
- Khalturin, V. I., Rautian, T. G., Richards, P. G., and Leith, W. S. (2005). A Review of Nuclear Testing by the Soviet Union at Novaya Zemlya, 1955–1990. *Sci. Glob. Security*. 13, 1–42. doi:10.1080/08929880590961862
- Khrennikov, D. E., Titov, A. K., Ershov, A. E., Pariev, V. I., and Karpov, S. V. (2020). On the Possibility of through Passage of Asteroid Bodies across the Earth's Atmosphere. *Mon. Notices R. Astron. Soc.* 493, 1344–1351. doi:10.1093/mnras/staa329
- Kilham, P. (1990). “Ecology of Melosira Species in the Great Lakes of Africa,” in *Large Lakes: Ecological Structure and Function*. Editors M. M. Tilzer and C. Serruya (Berlin: Springer-Verlag), 414–427. doi:10.1007/978-3-642-84077-7\_20
- Klaus, M., Karlsson, J., and Seekell, D. (2021). Tree Line advance Reduces Mixing and Oxygen Concentrations in Arctic-alpine Lakes through Wind Sheltering and Organic Carbon Supply. *Glob. Change Biol.* 27 (18), 4238–4253. doi:10.1111/gcb.15660
- Kletetschka, G., and Banerjee, S. K. (1995). Magnetic Stratigraphy of Chinese Loess as a Record of Natural Fires. *Geophys. Res. Lett.* 22 (11), 1341–1343. doi:10.1029/95GL01324
- Kletetschka, G., Kavková, R., Navrátil, T., Takáč, M., Prach, J., Vondrák, D., et al. (2019a). New Implications for Tunguska Explosion Based on Magnetic, Dendrological, and Lacustrine Records. *Meteorit. Planet. Sci.* 54 (S2), A206. doi:10.1111/maps.1334610.1029/95gl01324
- Kletetschka, G., Vondrák, D., Hrubá, J., van der Knaap, W. O., van Leeuwen, J. F. N., and Heurich, M. (2019b). Laacher See Tephra Discovered in the Bohemian Forest, Germany, East of the Eruption. *Quat. Geochronol.* 51, 130–139. doi:10.1016/j.quageo.2019.02.003
- Kletetschka, G., Procházka, V., Fantucci, R., and Trojek, T. (2017). Survival Response of *Larix Sibirica* to the Tunguska Explosion. *Tree-Ring Res.* 73 (2), 75–90. doi:10.3959/1536-1098-73.2.75
- Kletetschka, G., Vondrák, D., Hrubá, J., Procházka, V., Nabelek, L., Svitavská-Svobodová, H., et al. (2018). Cosmic-impact Event in lake Sediments from central Europe Postdates the Laacher See Eruption and marks Onset of the Younger Dryas. *J. Geology*. 126, 561–575. doi:10.1086/699869
- Kletetschka, G., Vyhnanek, J., Kawasumiova, D., Nabelek, L., and Petrucha, V. (2015). Localization of the Chelyabinsk Meteorite from Magnetic Field Survey and GPS Data. *IEEE Sensors J.* 15 (9), 4875–4881. doi:10.1109/JSEN.2015.2435252
- Kolesnikov, E. M., Kolesnikova, N. V., and Boettger, T. (1998). Isotopic Anomaly in Peat Nitrogen Is a Probable Trace of Acid rains Caused by 1908 Tunguska Bolide. *Planet. Space Sci.* 46 (2–3), 163–167. doi:10.1016/S0032-0633(97)00190-6
- Kolesnikov, E. M., Longo, G., Boettger, T., Kolesnikova, N. y. V., Gioacchini, P., Forlani, L., et al. (2003). Isotopic-geochemical Study of Nitrogen and Carbon in Peat from the Tunguska Cosmic Body Explosion Site. *Icarus*. 161, 235–243. doi:10.1016/S0019-1035(02)00024-6
- Kopáček, J., Evans, C. D., Hejzlar, J., Kaňa, J., Porcal, P., and Šantrůčková, H. (2018). Factors Affecting the Leaching of Dissolved Organic Carbon after Tree Dieback in an Unmanaged European Mountain forest. *Environ. Sci. Technol.* 52, 6291–6299. doi:10.1021/acs.est.8b00478
- Kopáček, J., Marešová, M., Hejzlar, J., and Norton, S. A. (2007). Natural Inactivation of Phosphorus by Aluminum in Preindustrial lake Sediments. *Limnol. Oceanogr.* 52 (3), 1147–1155. doi:10.4319/lo.2007.52.3.1147
- Kotov, A. A. (2016). Faunistic Complexes of the Cladocera (Crustacea, Branchiopoda) of Eastern Siberia and the Far East of Russia. *Biol. Bull. Russ. Acad. Sci.* 43 (9), 970–987. doi:10.1134/S1062359016090041
- Kresák, E. (1978). The Tunguska Object: A Fragment of Comet Encke? *Bull. Astr. Inst. Czechosl.* 29, 129–134.
- Kundt, W. (2001). The 1908 Tunguska Catastrophe: An Alternative Explanation. *Curr. Sci. India*. 81 (4), 399–407.
- Laing, T. E., and Smol, J. P. (2000). Factors Influencing Diatom Distributions in Circumpolar Treeline Lakes of Northern Russia. *J. Phycology*. 36, 1035–1048. doi:10.1046/j.1529-8817.2000.99229.x
- Lotter, A. F., Birks, H. J. B., Hofmann, W., and Marchetto, A. (1997). Modern Diatom, Cladocera, Chironomid, and Chrysophyte Cyst Assemblages as

- Quantitative Indicators for the Reconstruction of Past Environmental Conditions in the Alps. I. Climate. *J. Paleolimnol.* 18, 395–420. doi:10.1023/A:1007982008956
- Lotter, A. F., and Juggins, S. (1991). POLPROF, TRAN and ZONE: Programs for Plotting, Editing and Zoning Pollen and Diatom Data. *INQUA-Subcommission Study Holocene Working Group Data-Handling Methods Newsl.* 6, 4–6.
- Lotter, A. F., Pienitz, R., and Schmidt, R. (1999). "Diatoms as Indicators of Environmental Change Near Arctic and alpine Treeline," in *The Diatoms: Applications for the Environmental and Earth Sciences*. Editors E. F. Stoermer and J. P. Smol (Cambridge: Cambridge University Press), 205–226.
- Luoto, T. P. (2013). Dystrophy in Determining Midge Community Composition in Boreal Lakes. *Écoscience.* 20 (4), 391–398. doi:10.2980/20-4-3655
- Mackereth, F. J. H. (1966). Some Chemical Observations on post-glacial lake Sediments. *Phil. Trans. R. Soc. Lond. B.* 250, 165–213. doi:10.1098/rstb.1966.0001
- Massard, J. A., and Geimer, G. (2008). Global Diversity of Bryozoans (Bryozoa or Ectoprocta) in Freshwater. *Hydrobiologia.* 595, 93–99. doi:10.1007/s10750-007-9007-3
- Matisoff, G. (2017). Activities and Geochronology of 137 Cs in lake Sediments Resulting from Sediment Resuspension. *J. Environ. Radioactivity.* 167, 222–234. doi:10.1016/j.jenvrad.2016.11.015
- Melosh, H. J. (1989). *Impact Cratering: A Geologic Process*. New York: Oxford University Press.
- Moravcová, A., Tichá, A., Carter, V. A., Vondrák, D., Čtvrtliková, M., van Leeuwen, J. F., et al. (2021). Mountain Aquatic Isoetes Populations Reflect Millennial-Scale Environmental Changes in the Bohemian Forest Ecosystem, Central Europe. *The Holocene.* 31 (5), 746–759. doi:10.1177/0959683620988060
- Nazarova, L. B., Pestryakova, L. A., Ushnitskaya, L. A., and Hubberten, H.-W. (2008). Chironomids (Diptera: Chironomidae) in Lakes of central Yakutia and Their Indicative Potential for Paleoclimatic Research. *Contemp. Probl. Ecol.* 1 (3), 335–345. doi:10.1134/S1995425508030089
- Norton, S. A., Perry, R. H., Saros, J. E., Jacobson, G. L., Jr., Fernandez, I. J., Kopáček, J., et al. (2011). The Controls on Phosphorus Availability in a Boreal lake Ecosystem since Deglaciation. *J. Paleolimnol.* 46, 107–122. doi:10.1007/s10933-011-9526-9
- Pleskot, K., Tjallingii, R., Makohonienko, M., Nowaczyk, N., and Szczuciński, W. (2018). Holocene Paleohydrological Reconstruction of Lake Strzeszyńskie (Western Poland) and its Implications for the central European Climatic Transition Zone. *J. Paleolimnol.* 59, 443–459. doi:10.1007/s10933-017-9999-2
- Ponomarev, E., Ponomareva, T., Masyagina, O., Shvetsov, E., Ponomarev, O., Krasnoshchekov, K., et al. (2019). Post-fire Effect Modeling for the Permafrost Zone in Central Siberia on the Basis of Remote Sensing Data. *Proceedings.* 18 (1), 6. doi:10.3390/ECRS-3-06202
- Rapuc, W., Jacq, K., Develle, A.-L., Sabatier, P., Fanget, B., Perrette, Y., et al. (2020). XRF and Hyperspectral Analyses as an Automatic Way to Detect Flood Events in Sediment Cores. *Sediment. Geology.* 409, 105776. doi:10.1016/j.sedgeo.2020.105776
- Rieradevall, M., and Brooks, S. J. (2001). An Identification Guide to Subfossil Tanytopodinae Larvae (Insecta: Diptera: Chironomidae) Based on Cephalic Setation. *J. Paleolimnol.* 25 (1), 81–99. doi:10.1023/A:1008185517959
- Robertson, D. K., and Mathias, D. L. (2019). Hydrocode Simulations of Asteroid Airbursts and Constraints for Tunguska. *Icarus.* 327, 36–47. doi:10.1016/j.icarus.2018.10.017
- Rogozin, D. Y., Darin, A. V., Kalugin, I. A., Melgunov, M. S., Meydus, A. V., and Degermendzhi, A. G. (2017). Sedimentation Rate in Cheko Lake (Evenkia, Siberia): New Evidence on the Problem of the 1908 Tunguska Event. *Dokl. Earth Sc.* 476 (2), 1226–1228. doi:10.1134/S1028334X17100269
- Rosanna, F., Romano, S., Gunther, K., and Mario, D. (2015). The Tunguska Event and Cheko lake Origin: Dendrochronological Analysis. *Int. J. Astrobiology.* 14 (3), 345–357. doi:10.1017/S1473550414000445
- Round, F. E., Crawford, R. M., and Mann, D. G. (1990). *The Diatoms: Biology and Morphology of the Genera*. Cambridge: Cambridge University Press.
- Saunders, K. M., Hodgson, D. A., and McMinn, A. (2009). Quantitative Relationships between Benthic Diatom Assemblages and Water Chemistry in Macquarie Island Lakes and Their Potential for Reconstructing Past Environmental Changes. *Antarctic Sci.* 21 (1), 35–49. doi:10.1017/S0954102008001442
- Shishkin, N. I. (2007). Seismic Efficiency of a Contact Explosion and a High-Velocity Impact. *J. Appl. Mech. Tech. Phys.* 48 (2), 145–152. doi:10.1007/s10808-007-0019-6
- Smol, J. P. (1988). Paleoclimate Proxy Data from Freshwater Arctic Diatoms. *SIL Proc.* 23, 837–844. doi:10.1080/03680770.1987.11899722
- Solomon, C. T., Jones, S. E., Weidel, B. C., Buffam, I., Fork, M. L., Karlsson, J., et al. (2015). Ecosystem Consequences of Changing Inputs of Terrestrial Dissolved Organic Matter to Lakes: Current Knowledge and Future Challenges. *Ecosystems.* 18, 376–389. doi:10.1007/s10021-015-9848-y
- Stanghellini, G., and Carrara, G. (2017). Segy-change: The Swiss Army Knife for the SEG-Y Files. *SoftwareX.* 6, 42–47. doi:10.1016/j.softx.2017.01.003
- Svetsov, V. V. (2002). Comment on "Extraterrestrial Impacts and Wildfires". *Palaeogeogr. Palaeoclimatol. Palaeoecol.* 185, 403–405. doi:10.1016/S0031-0182(02)00341-3
- Szeroczyńska, K., and Sarmaja-Korjonen, K. (2007). *Atlas of Subfossil Cladocera from Central and Northern Europe*. Swiecie: Friends of the Lower Vistula Society.
- Tchepakova, N. M., Parfenova, E. I., and Soja, A. J. (2011). Climate Change and Climate-Induced Hot Spots in forest Shifts in central Siberia from Observed Data. *Reg. Environ. Change.* 11 (4), 817–827. doi:10.1007/s10113-011-0210-4
- Tichá, A., Bešta, T., Vondrák, D., Houfková, P., and Jankovská, V. (2019). Nutrient Availability Affected Shallow-lake Ecosystem Response along the Late-Glacial/Holocene Transition. *Hydrobiologia.* 846 (1), 87–108. doi:10.1007/s10750-019-04054-7
- Toon, O. B., Zahnle, K., Morrison, D., Turco, R. P., and Covey, C. (1997). Environmental Perturbations Caused by the Impacts of Asteroids and Comets. *Rev. Geophys.* 35 (1), 41–78. doi:10.1029/96RG03038
- Tositti, L., Mingozzi, M., Sandrini, S., Forlani, L., Buoso, M., Depoli, M., et al. (2006). A Multitracer Study of Peat Profiles from Tunguska, Siberia. *Glob. Planet. Change.* 53 (4), 278–289. doi:10.1016/j.gloplacha.2006.03.010
- Turco, R. P., Toon, O. B., Park, C., Whitten, R. C., Pollack, J. B., and Noerdlinger, P. (1981). Tunguska Meteor Fall of 1908: Effects on Stratospheric Ozone. *Science.* 214 (4516), 19–23. doi:10.1126/science.214.4516.19
- Wiederholm, T. (1983). Chironomidae of the Holarctic Region: Keys and Diagnoses. Part 1. Larvae. *Entomol. Scand. Suppl.* 19, 1–457.
- Ursenbacher, S., Stötter, T., and Heiri, O. (2020). Chitinous Aquatic Invertebrate Assemblages in Quaternary lake Sediments as Indicators of Past deepwater Oxygen Concentration. *Quat. Sci. Rev.* 231, 106203. doi:10.1016/j.quascirev.2020.106203
- van der Werff, A. (1953). A New Method of Concentrating and Cleaning Diatoms and Other Organisms. *SIL Proc.* 12, 276–277. doi:10.1080/03680770.1950.11895297
- Vasconcelos, F. R., Diehl, S., Rodríguez, P., Hedström, P., Karlsson, J., and Byström, P. (2016). Asymmetrical Competition between Aquatic Primary Producers in a Warmer and Browner World. *Ecology.* 97 (10), 2580–2592. doi:10.1002/ecy.1487
- Vasilyev, N. V. (1998). The Tunguska Meteorite Problem Today. *Planet. Space Sci.* 46 (2/3), 129–150. doi:10.1016/S0032-0633(97)00145-1
- Weather and Climate (2021). Vanavara. Available at: <http://www.pogodaiklimat.ru/history/24908.htm> (Accessed August 10, 2021).
- Westover, K. S., Fritz, S. C., Blyakharchuk, T. A., and Wright, H. E. (2006). Diatom Paleolimnological Record of Holocene Climatic and Environmental Change in the Altai Mountains, Siberia. *J. Paleolimnol.* 35 (3), 519–541. doi:10.1007/s10933-005-3241-3
- Wilhelm, B., Vogel, H., and Anselmetti, F. S. (2017). A Multi-Centennial Record of Past Floods and Earthquakes in Valle d'Aosta, Mediterranean Italian Alps. *Nat. Hazards Earth Syst. Sci.* 17, 613–625. doi:10.5194/nhess-17-613-2017
- Włodarski, W., Papis, J., and Szczuciński, W. (2017). Morphology of the Morasko Crater Field (Western Poland): Influences of Pre-impact Topography, Meteoroid Impact Processes, and post-impact Alterations. *Geomorphology.* 295, 586–597. doi:10.1016/j.geomorph.2017.08.025
- Wolfe, A. P. (2003). Diatom Community Responses to Late-Holocene Climatic Variability, Baffin Island, Canada: a Comparison of Numerical Approaches. *The Holocene.* 13, 29–37. doi:10.1191/0959683603hl592rp
- Wünnemann, K., and Weiss, R. (2015). The Meteorite Impact-Induced Tsunami hazard. *Phil. Trans. R. Soc. A.* 373, 20140381. doi:10.1098/rsta.2014.0381

- Xu, H., Liu, B., and Wu, F. (2010). Spatial and Temporal Variations of Rb/Sr Ratios of the Bulk Surface Sediments in Lake Qinghai. *Geochem. Trans.* 11, 3. doi:10.1186/1467-4866-11-3
- Zaslavskaya, N. I., Zotkin, I. T., and Kirova, O. A. (1964). Size Distribution of Magnetite Globules from Outer Space, Found in the Soil of the Region where the Tunguska Meteorite Has Fallen. *Dokl. Akad. Nauk SSSR.* 156 (1), 47–49.
- Zhang, C., Qiao, Q., Piper, J. D. A., and Huang, B. (2011). Assessment of Heavy Metal Pollution from a Fe-Smelting Plant in Urban River Sediments Using Environmental Magnetic and Geochemical Methods. *Environ. Pollut.* 159, 3057–3070. doi:10.1016/j.envpol.2011.04.006

**Conflict of Interest:** The authors declare that the research was conducted in the absence of any commercial or financial relationships that could be construed as a potential conflict of interest.

**Publisher's Note:** All claims expressed in this article are solely those of the authors and do not necessarily represent those of their affiliated organizations, or those of the publisher, the editors and the reviewers. Any product that may be evaluated in this article, or claim that may be made by its manufacturer, is not guaranteed or endorsed by the publisher.

Copyright © 2022 Kavková, Vondrák, Chattová, Svecova, Takac, Golias, Štorc, Stanghellini and Kletetschka. This is an open-access article distributed under the terms of the Creative Commons Attribution License (CC BY). The use, distribution or reproduction in other forums is permitted, provided the original author(s) and the copyright owner(s) are credited and that the original publication in this journal is cited, in accordance with accepted academic practice. No use, distribution or reproduction is permitted which does not comply with these terms.